

REVISED — LENDING PANE LP 388(CULL)



London Road, Bracknell
Berkshire RG12 2SZ

LONDON, METEOROLOGICAL OFFICE.
Met.O.11 Technical Note No.254

Numerical modelling of balanced atmospheric flow.

06550787

FGZ

National Meteorological Library
and Archive

Archive copy - reference only

SL & R.

(287)

METEOROLOGICAL OFFICE
150587
24 JUL 1987
LIBRARY c

MET O 11 TECHNICAL NOTE NO 254

NUMERICAL MODELLING OF BALANCED ATMOSPHERIC FLOW

M.J.P. Cullen & G.J. Shutts

Met O 11 (Forecasting Research),
Meteorological Office,
London Road,
Bracknell,
Berkshire,
England.

April 1987.

N.B This paper has not been published. Permission to quote from it
must be obtained from the Assistant Director of the above Met
Office Branch.

FH2A

METEOROLOGICAL OFFICE
LIBRARY
24 JUL 1985

281

NET 0 11 TECHNICAL NOTE NO 281

NUMERICAL MODELLING OF BALANCED ATMOSPHERIC FLOW

M.J.P. Cullen & G.J. Shutts

NET 0 11 TECHNICAL NOTE NO 281
METEOROLOGICAL OFFICE
LONDON ROAD
BRACKNELL
BERKSHIRE
ENGLAND

APRIL 1987

This paper has not been published. It is available to those who can be obtained from the Assistant Director of the above for Office Branch

NUMERICAL MODELLING OF BALANCED ATMOSPHERIC FLOW

M.J.P. Cullen and G.J. Shutts

Meteorological Office,
Bracknell, Berks., U.K.

NUMERICAL MODELLING OF BALANCED ATMOSPHERIC FLOW

M. J. Cullen and G. J. Storer

Meteorological Office

Bracknell, Berks, U.K.

1. INTRODUCTION

ABSTRACT

Atmospheric flows of importance for weather forecasting are mostly characterised by a requirement of 'balance' in which the three-dimensional wind field can be determined implicitly from the pressure and moisture distribution. A mathematical definition of balance is described based on a Hamiltonian formulation which requires that sufficiently large fluid parcels remain close to a minimum energy configuration. The resulting evolution equations are an approximate form of the equations of motion. Numerical solutions of the equations describing balanced flow are presented and compared with those where the balance approximation is not enforced. There are large differences in cases where the balanced equations have singular solutions. The implications for modelling real atmospheric flows are discussed.

Key words

It is first necessary to establish what is meant by 'balanced' flows. In the context of weather forecasting, the term 'balanced' is used to describe flows which are well represented by the quasi-geostrophic approximation. This approximation is based on the assumption that the time scale of the motion is much longer than the time scale of the rotation of the Earth. In this approximation, the vertical motion is determined by the continuity equation, and the horizontal motion is determined by the geostrophic balance. The resulting equations are the quasi-geostrophic equations. These equations are a simplification of the full equations of motion, and are used to describe the large-scale motion of the atmosphere. The quasi-geostrophic approximation is valid for most weather systems, but it fails for some systems, such as those with strong vertical shear or those with strong curvature. In these cases, the full equations of motion must be used. The full equations of motion are a set of partial differential equations, and are difficult to solve. Numerical solutions of the full equations of motion are presented and compared with those where the balance approximation is not enforced. There are large differences in cases where the balanced equations have singular solutions. The implications for modelling real atmospheric flows are discussed.

ABSTRACT

1. INTRODUCTION

This paper discusses a strictly mathematical approach to the problem of numerical weather prediction. In many areas of computational fluid mechanics, it is becoming widely recognised that knowledge of the mathematical properties of the desired solution is essential for successful computations. A number of recent numerical methods are realisations of proofs of the existence and uniqueness of solutions to the governing equations and are thus guaranteed to converge to those solutions as the resolution of the calculations is increased. The most common example of such methods is the finite element method for elliptic boundary value problems. Temam(1977) describes this relationship for the Navier-Stokes equations. Majda(1986) shows how this philosophy can be applied to computing three dimensional incompressible flows at high Reynolds number.

It is first necessary to determine what types of atmospheric motions are associated with weather. If the weather is to be predictable, then these motions must evolve independently of other atmospheric motions. In practice there can at most be partial independence; however the achievement of quite accurate numerical forecasts for up to five days ahead indicates a high degree of predictability in practice (WMO 1986). Lorenz(1969) showed that one way of achieving this requires a "spectral gap" so that large scale motions can evolve independently of small scale detail. Observational studies do not support the existence of a "spectral gap" (Lilly 1982). Predictability can be achieved, however, if there are stable coherent structures in the atmosphere which evolve almost independently of other motions (Lorenz 1984).

In order to achieve the maximum predictability in a computer simulation, we must first define a subset of atmospheric motions which we expect to evolve independently: this can be done in terms of horizontal and vertical scale. The complete Navier-Stokes equations are integrated, together with whatever forcing terms are necessary. A grid, or spectral truncation, sufficient to represent the desired scales accurately is chosen and smaller scales which can be resolved, but not accurately treated, are filtered out. Such procedures are described in standard textbooks on numerical weather prediction, e.g. Haltiner and Williams(1980), Pielke(1984). It is found that a definition purely in terms of spatial scale is not sufficient and that the time scale must also be restricted. Browning and Kreiss (1985) derive conditions under which solutions of the Navier-Stokes equations for the atmosphere will vary slowly in time and find it necessary to require smooth vertical structure. This is too restrictive an assumption to describe atmospheric structures associated with significant weather which are often almost discontinuous.

Cullen et al. (1987) attempted to remove this restriction by characterising weather-producing motions as solutions of a set of Lagrangian equations derived from considering the average motion of fluid parcels and requiring those parcels to remain close to a minimum energy configuration. The equations obtained are one of many different types of "filtered equations" developed by dynamical meteorologists to describe subsets of atmospheric motions relevant to weather. The solutions obtained from that model can be discontinuous and can also allow fluid parcels to jump discontinuously between two equilibrium positions. They cannot be obtained by integrating the Navier-Stokes

equations numerically in a way that forces the solution to stay smooth. The equations are a strong candidate for describing an independent subset of atmospheric motions for two reasons. They contain no horizontal derivatives in the evolution equations. The only derivatives are rates of change following fluid parcels. They therefore do not rely on possibly unrepresentative estimates of spatial derivatives in the atmosphere. Secondly, in two-dimensional flow, the minimum energy configuration can be predicted independently of the remainder of the flow provided there is no mixing. In three dimensions, the minimum energy configuration can only be affected by non-equilibrium motions in a significant proportion of the fluid. Other systems of filtered equations, for instance those reviewed by Gent and McWilliams(1983), appear to break down if the assumptions used to derive them fail anywhere in space.

In this paper we discuss how the theory of Cullen et al. can be applied to practical numerical weather prediction. The system of equations is implicit and nonlinear. It is possible to use Lagrangian numerical methods to solve them in special cases. This allows exact solutions to be obtained. However for practical simulations it appears necessary to use Eulerian numerical methods on a fixed grid, or spectral truncation. Iterative methods of solving the implicit equations are described here. Similar implicit problems have to be solved in steady flow simulations in engineering. It is well known, however, that it is often easier to solve them by integrating time-dependent equations to a steady state. An analogy in the weather prediction problem would be to follow the slowly varying solution predicted by the implicit nonlinear equations by integrating a more general set of equations in which the

time dependence is explicit. This corresponds to the standard method of designing weather prediction models where the spatially-averaged Navier-Stokes equations are integrated in such a way that a slowly varying solution is produced. We compare the two approaches.

Section 2 describes the mathematical model of Cullen et al. and the solutions it gives. A case in which the solution exhibits singular behaviour is illustrated. Section 3 describes finite difference methods for approximating the solutions and compares them with finite difference procedures used to solve the more general explicit equations. Section 4 gives illustrative results and Section 5 discusses practical implications.

2. MATHEMATICAL MODEL

2.1 General principles

The conventional approach to numerical weather prediction starts from the compressible Navier-Stokes equations in an appropriate coordinate system and then derives averaged equations appropriate to the scales being resolved by Eulerian Reynolds averaging, Pielke (1984). Descriptive texts on weather, however, find it more natural to use a Lagrangian description and discuss the behaviour of air masses. Thus thunderstorms can be forecast by identifying situations where cold, dry air flows over warm, moist air resulting in convective instability of the air column. The mathematical model used here averages the equations over air parcels: the parcels are then assumed to be sufficiently large that they can be assumed to remain at all times in a minimum energy configuration. This assumption excludes most types of transient wave motions such as gravity or inertial waves. Observations suggest that most of the energy in such waves is concentrated in scales

not normally resolved by weather forecasting models and that they rarely have a direct effect on the actual weather as described in a forecast. Such motions, however determine the shapes of individual clouds.

2.2 Variational formulation

The equations are first derived for motions in a three dimensional system rotating with angular velocity Ω in the presence of a gravitational potential Π . The energy of the fluid can be written as

$$E = \int d\Gamma [\frac{1}{2}|\underline{v}|^2 + U + \Pi] \quad (2.1)$$

In this expression $d\Gamma$ represents a volume increment $dadbc$ in particle label space (a,b,c) (alternatively it can be regarded as a mass increment), U is the internal energy of the fluid and can be written $U(\alpha,s)$, where α is the specific volume and S the entropy. (u,v,w) represent velocity components. Shutts and Cullen (1987) derive conditions for the energy to be stationary with respect to infinitesimal particle displacements. The displacements χ are assumed to be instantaneous and adiabatic so that the entropy is conserved. In such a displacement in a rotating system the velocity components except the component parallel to the axis of rotation will change due to the Coriolis effect. Shutts and Cullen show that the resulting equation is

$$\delta V = - 2\Omega \times \chi \quad (2.2)$$

The change in E due to the displacement is then

$$\delta E = \int [\delta(\frac{1}{2}|\underline{v}|^2) + C_v \delta T + \delta \Pi] \quad (2.3)$$

T is the temperature and C_v the specific heat of air at constant volume. Since $\delta\Pi$ is the change in geopotential energy experienced by a parcel during a displacement we have

$$\delta\Pi = \chi \cdot \nabla\phi.$$

The continuity equation for a perfect gas and the first law of thermodynamics for an adiabatic displacement are then used to give

$$C_v \delta T = -p \delta \alpha = -p \alpha \nabla \cdot \chi$$

Equation (2.2) is used to show that

$$\delta(\frac{1}{2} |v|^2) = \mathbf{v} \cdot \delta \mathbf{v} = \chi \cdot (2\mathbf{Q} \times \mathbf{v})$$

and equation (2.3) can then be written:

$$\int d\Gamma [\chi \cdot (2\mathbf{Q} \times \mathbf{v} + \nabla\phi) - \alpha p \nabla \cdot \chi] \quad (2.4)$$

Assuming zero normal displacement at rigid boundaries and the vanishing of $p\chi$ at the top of a compressible atmosphere, the condition for an extremum is

$$2\mathbf{Q} \times \mathbf{v} + \nabla\phi + \alpha \nabla p = 0 \quad (2.5)$$

This is a general statement of geostrophic and hydrostatic balance. If this condition is applied to the atmosphere, it includes the conventional geostrophic relation for the wind components normal to the gravitational force- in other words the horizontal wind. It gives no information about the northward component of wind at the equator since this component is parallel to the axis of rotation. The component of (2.5) normal to the earth's surface includes the conventional hydrostatic relation with an extra term from $2\mathbf{Q} \times \mathbf{v}$ which is negligible relative to $\nabla\phi$.

Shutts and Cullen show that the condition for this stationary point to be a minimum is

$$\chi \cdot \mathbf{Q} \cdot \chi \geq 0 \quad (2.6)$$

where

$$\mathbf{Q} = 2\mathbf{Q}\mathbf{v}\mathbf{M} - \alpha \nabla S \nabla p \quad (2.7)$$

$$\mathbf{M} = 2\mathbf{Q}(\mathbf{r} - (\mathbf{Q} \cdot \mathbf{r})\mathbf{Q}/\Omega^2) - \mathbf{Q} \times \mathbf{v}/\Omega \quad (2.8)$$

and \mathbf{r} is a position vector. These conditions for a minimum energy state thus require the horizontal wind to be geostrophic and the vertical pressure distribution to be hydrostatic.

In order to make forecasts it is necessary to find equations for the time evolution of the atmosphere using the assumption that it is close to a minimum energy state. Salmon(1985) derives evolution equations from Hamilton's principle though he does not connect his treatment with energy minimisation. We give a slightly different Hamiltonian formulation based on the energy arguments. This is described in detail by Shutts(1987). The Hamiltonian for general motions is given by

$$H = \int d\Gamma [\frac{1}{2}(u^2+v^2+w^2) + U + \phi - p_0(J((x,y,z)/(a,b,c) - \alpha) - T_0(S - S_0))], \quad (2.9)$$

where (u,v,w) are velocity components in a Cartesian frame (x,y,z) oriented so that the z direction is parallel to the axis of rotation, $S_0(a,b,c)$ is the initial entropy and p_0, T_0 are Lagrange multipliers. The evolution is then governed by an action principle

$$\delta \int_{(t_0, t_1)} d\tau \left\{ \int d\Gamma \left[(u - \Omega y) \frac{\delta x}{\delta \tau} + (v + \Omega x) \frac{\delta y}{\delta \tau} + w \frac{\delta z}{\delta \tau} \right] d\Gamma - H(\tau) \right\} = 0 \quad (2.10)$$

where variations taken with respect to x, y, z, u, v, w, α and S are considered to be independent (c.f. Salmon 1987).

Variations with respect to x, y and z give the Euler equations of motion; variations with respect to u, v and w give the definitions $u = \delta x / \delta \tau$ required for consistency and the variations with respect to α and S provide the thermodynamic definitions of pressure and temperature in terms of internal energy.

We now wish to restrict the action principle to deal with motions close to minimum energy. This is done by making two approximations. The first is to neglect the kinetic energy of the component of motion parallel to the axis of rotation and the corresponding term in the action integral. We then transform the principle into canonical coordinates. Define

$$\begin{aligned} M &= 2\Omega x + v \\ N &= 2\Omega y - u \end{aligned} \quad (2.11)$$

from components of (2.8). Then Shutts (1987) proposes the following approximation to the Hamiltonian:

$$\begin{aligned} H &= \int d\Gamma \left[\frac{1}{2} (2\Omega y - N)^2 + \frac{1}{2} (M - 2\Omega x)^2 + U + \phi - p_0 (J(x, y, z) / (a, b, c) - \alpha) \right. \\ &\quad \left. - T_0 (S - S_0) \right] \end{aligned} \quad (2.12)$$

This involves the neglect of a term $|\delta \beta / \delta \tau| / 2\Omega$ as $\ll 1$, where β is the wind direction measured as an angle from a reference direction. The action principle becomes

$$\delta \int_{(t_0, t_1)} d\tau \left\{ \int d\Gamma \left[M \frac{\delta N}{\delta \tau} - N \frac{\delta M}{\delta \tau} \right] / 4\Omega - H(\tau) \right\} = 0 \quad (2.13)$$

Variations with respect to x, y and z give

$$\delta x: -2\Omega (M - 2\Omega x) + \delta \phi / \delta x + \alpha \delta p / \delta x = 0 \quad (2.14)$$

$$\delta y: 2\Omega(2\Omega y - N) + \delta\phi/\delta y + \alpha\delta p/\delta y = 0 \quad (2.15)$$

$$\delta z: \delta\phi/\delta z + \alpha\delta p/\delta z = 0 \quad (2.16)$$

These are the geostrophic and hydrostatic relations (2.5), showing that the approximate Hamiltonian is indeed associated with motions close to minimum energy. The evolution equations are obtained from variations with respect to M and N:

$$\delta M: \delta N/\delta\tau/2\Omega - (M - 2\Omega x) = 0 \quad (2.17)$$

$$\delta N: -\delta M/\delta\tau/2\Omega + (2\Omega y - N) = 0 \quad (2.18)$$

It can be shown that in the special case where $\nabla\phi$ is parallel to the axis of rotation the equations are exactly the semi-geostrophic equations derived by Hoskins(1975) by replacing the actual momentum by its geostrophic value in the unapproximated equations of motion. These equations conserve the energy given by (2.12). Salmon(1985) derived a similar set of equations to (2.14)-(2.18) from a slightly different Hamiltonian formulation.

The remaining equations to close the problem are not approximated and are given by the constraints:

$$J((x, y, z)/(a, b, c)) = \alpha \quad (2.19)$$

$$S = S_0(a, b, c) \quad (2.20)$$

and the variation with respect to α :

$$p = -\delta U/\delta\alpha \quad (2.21)$$

together with a knowledge of the function $U(\alpha, S)$ for a perfect gas.

The system of equations (2.17) to (2.21) contains no spatial derivatives. The definitions (2.14) to (2.16) require the

pressure to be differentiable but do not require that M and N are continuous. Since it is only necessary to know M, N and S for fluid parcels which fill the total available volume, the requirement on the pressure can be relaxed to differentiability almost everywhere; with M, N and S undefined on a set of measure zero.

2.3 Properties of solutions

It is simplest to explain the properties of this model by examining a two-dimensional version. Consider a domain in the (x, z) plane with rigid boundaries. Following Hoskins(1975) write the equations using a vertical coordinate which is a specially chosen function of pressure so that the equations transform into a set like those for an incompressible fluid. The unapproximated equations are then

$$Du/Dt + \delta\phi/\delta x - 2\Omega v = 0 \quad (2.22)$$

$$Dv/Dt + 2\Omega u = 0 \quad (2.23)$$

$$Dw/Dt + \delta\phi/\delta z - ge^S = 0 \quad (2.24)$$

$$DS/Dt = 0 \quad (2.25)$$

$$D\alpha/Dt = 0 \quad (2.26)$$

$$u \cdot n = 0 \text{ on boundaries.} \quad (2.27)$$

Any solution of these equations is an area-preserving rearrangement of the fluid, because of (2.26) and (2.27). The rearrangement preserves the entropy S and the absolute momentum $M \equiv (v + 2\Omega x)$ following fluid parcels. The energy that can be attained in such a rearrangement is stationary when the geostrophic and hydrostatic relations (2.5) are satisfied. For this problem (2.5) takes the form:

$$\delta\phi/\delta x = 2\Omega v \quad (2.28)$$

$$\delta\phi/\delta z = ge^S \quad (2.29)$$

The condition (2.6) for this arrangement to give a minimum of the energy becomes

$$(\partial M / \partial x)(\partial S / \partial z) - (\partial M / \partial z)(\partial S / \partial x) \geq 0 \quad (2.30)$$

$$\partial S / \partial z \geq 0.$$

Given general initial data not satisfying (2.28) and (2.29), the total energy will be conserved and the solution will not be able to reach minimum energy. If a dissipative mechanism for u and w is included but no mixing of M and S allowed, the solution will tend asymptotically to that of the system (2.23), (2.25)-(2.29). This reduced system is the two-dimensional version of the approximate equations (2.17)-(2.21). As written so far, they describe a steady unidirectional flow in geostrophic and hydrostatic balance. A non-trivial problem can be obtained by specifying source terms, for instance by including a basic pressure gradient in the y direction and including effects that can change the entropy of fluid parcels. We illustrate this with a model of moist frontogenesis developed by Holt (1987). The equations are:

$$\partial \phi / \partial x = 2\Omega v \quad (2.31)$$

$$\partial \phi / \partial z = g e^{\sigma} \quad (2.32)$$

$$DM/Dt \equiv D(v+2\Omega x)/Dt = -\sigma M \quad (2.33)$$

$$\begin{aligned} DS/Dt &= LDq/Dt & q > q_{*} &) \\ &= 0 & q < q_{*} &) \end{aligned} \quad (2.34)$$

$$\begin{aligned} Dq/Dt &= 0 & q < q_{*} &) \\ &= Dq_{*}/Dt & q > q_{*} &) \end{aligned} \quad (2.35)$$

$$DA/Dt = -\sigma A \quad (2.36)$$

$$u \cdot n = 0 \text{ on boundaries.} \quad (2.37)$$

These equations are to be solved in a region of the (x,z) plane which shrinks laterally with time, its area being proportional to $e^{-\sigma t}$. A is the specific cross-section of the air. The extra variable q represents the moisture content of the air, q_{*} is the saturation moisture content, and L the latent heat of evaporation. Figs. 1 and 2 illustrate a solution. The data is approximated by a piecewise constant distribution of M, S and q . The solution will then remain piecewise constant when integrated in time, provided that a single value of q_{*} is used for each element. Cullen and Purser (1984) prove that the equations have a unique piecewise constant solution which satisfies the stability condition (2.30).

In the solution shown Fig. 1 illustrates the initial data. The moisture content is greatest in the parcels nearest the bottom boundary. The solution then evolves under a basic state deformation field which enters through the source terms in (2.33) and (2.36). A discontinuity corresponding to an atmospheric front forms at the lower boundary: this is a contact discontinuity which no fluid crosses. Parcels initially in contact with the lower boundary separate from it. The value of q_{*} for a parcel depends on the pressure and decreases as it ascends. Some of the parcels which are forced off the lower boundary increase their values of S according to (2.34) sufficiently to violate (2.30) and jump discontinuously to a position in the upper atmosphere as is shown in Fig. 2.

The meteorological justification for these solutions is discussed by Cullen et al. (1987). In mathematical terms they are strong solutions of the Lagrangian equations because M, S and q vary continuously following fluid parcels. However, if fronts form, u and w

are discontinuous though energy is still conserved. If parcels jump, u and w are undefined and a well-defined amount of energy is dissipated. These solutions are not likely to be solutions of the Eulerian form of the equations, even in a weak sense; numerical solution by conventional methods will therefore be very difficult. The rest of this paper considers how finite difference methods on a fixed mesh can be used to solve the problem. The fully Lagrangian method used to generate the solution in Figs. 1 and 2 is inherently first order accurate at best and does not at present appear practicable for operational weather forecasting models.

2.4 Relation to other mathematical models

The model described above is only one of a wide variety that have appeared in the meteorological literature which distinguish weather-producing motions from other atmospheric motions. Our model is based on the geostrophic approximation to the horizontal wind and therefore does not allow any horizontal pressure gradient along the equator except across mountains. An alternative, Gent and McWilliams (1983), is to expand the horizontal velocity in its rotational and divergent components, and, for instance, replace the momentum by that of the rotational component. The pressure distribution has to be determined implicitly. The rotational component of the horizontal wind has to satisfy a constraint which ensures that this implicit problem is elliptic, analogous to the condition (2.6) in our model. Their type of formulation does not appear so restrictive near the equator, but the decomposition into rotational and divergent components relies on the smoothness of the horizontal velocity in space. It is not at all clear whether it can be generalised to make sense for discontinuous phenomena

such as fronts, or the convecting solution illustrated above. Different types of weather are important at low latitudes and it would not be surprising if different approximate formulations were needed there.

In operational forecast models, it is most common to distinguish weather-producing motions in terms of normal modes. The unapproximated equations are represented as a finite-dimensional system using finite difference, finite element or spectral methods. This system is linearised about a state of rest and normal modes of the resulting equations calculated. These modes may correspond to sound waves, gravity waves, or slowly propagating waves associated with weather systems. The initial data is then prepared by requiring the initial time tendencies of the unwanted modes to be small or zero. Two ways of doing this are normal mode initialisation, (Temperton and Williamson, 1979), and the bounded derivative method, (Browning and Kreiss, 1985). The latter paper shows rigorously that the procedure only makes sense if the vertical structure is smooth because only then is the linearisation about a state of rest reasonable. It is again difficult to see how this procedure makes sense in the presence of discontinuities or convection.

A simpler procedure used, for instance, in some of the operational models at the U.K. Meteorological Office, Gadd (1985), is to add selective diffusion of the divergent component of the horizontal wind. In the two-dimensional problem discussed in section 2.3 this allows the system to reach the minimum energy configuration described there since only u and w would be diffused. In three dimensions, however, this technique would give a different solution from our model since it is based on the divergent rather than the ageostrophic wind.

3. METHODS OF SOLUTION

3.1 Solution of the semi-geostrophic equations

We first set out a solution procedure for the system (2.23), (2.25)-(2.29). The procedure is designed so that it can readily be applied to a three-dimensional model by using an alternating direction method. The aim in this paper is to relate the procedure to methods of solving the unapproximated equations (2.22)-(2.27). Only the detail needed to make the comparison is therefore given; a much fuller description is given by Cullen (1987). A second order finite difference algorithm is described. A similar procedure could be developed using higher order finite difference methods, finite element, or spectral methods.

The first requirement is to set up the grid to represent the geostrophic and hydrostatic relations (2.28) and (2.29) in the most natural way. This suggests that S , ϕ and v are arranged on the grid as shown in Fig. 3. Equation (2.26) is then replaced by its Eulerian form

$$\partial u / \partial x + \partial w / \partial z = 0 \quad (3.1)$$

We will use a rectangular domain $-L \leq x \leq L, 0 \leq z \leq H$. The boundary conditions (2.27) then become

$$\begin{aligned} u &= 0 \text{ at } x = \pm L \\ w &= 0 \text{ at } z = 0, H. \end{aligned} \quad (3.2)$$

These equations suggest the arrangement of u and w on the grid shown in Fig. 3. Note that if the grid has N layers between the upper and lower boundaries, there are $(N-1)$ independent values of w that can be computed for each value of x . This number has to match the number of constraints that have to be enforced between the v and S fields. These constraints can be written

$$2\Omega \partial v / \partial z = g e^{\phi} \partial S / \partial x. \quad (3.3)$$

The form of this constraint suggests the arrangement of v and S on the grid shown in Fig. 3. There can only be $(N-1)$ values of S in each column. This grid arrangement can be easily extended to a three-dimensional model.

The procedure for advancing the solution for one timestep consists of four stages. Equations (2.23) and (2.25) are stepped forward in time:

$$v' = v^0 - (u \cdot \nabla v + 2\Omega u) \Delta t \quad (3.4)$$

$$S' = S^0 - (u \cdot \nabla S) \Delta t \quad (3.5)$$

The operator $u \cdot \nabla$ denotes $u \partial / \partial x + w \partial / \partial z$. The values of u appearing on the right hand sides of (3.4) and (3.5) are those at time level 0. Those of S and v can be averages of values at time levels 0 and 1. Any forcing terms, such as that in (2.34), are also added at this stage. v' and S' will not satisfy (3.3). Before imposing this constraint by calculating a new value of u and correcting v' and S' , it is necessary to enforce (2.30) on the values at time level 1. If this condition is not satisfied the equation for the new value of u will not be elliptic. It is very difficult to enforce (2.30) without somewhere creating values of S and v out of the range present in the original data. Since (2.25) states that S is at all times a rearrangement of the initial data, this is undesirable and may lead to computational instability. A simpler procedure is therefore followed. The values of S in each vertical column are adjusted so that $\partial S / \partial z > 0$. The adjustment conserves the vertical integral of S and imposes zero gradient in regions of negative gradient. The values of $(v+2\Omega x)$ are similarly adjusted so that $\partial (v+2\Omega x) / \partial x > 0$. These conditions are implied by (2.30) but are not

sufficient to satisfy it. Write the values of S and v after adjustment as S^2, v^2 .

S^2, v^2 are now corrected to satisfy (3.3), by calculating a new u field u^2 that satisfies (3.1) and (3.2). The calculation is performed using a subset of equations (3.4) and (3.5), namely

$$v^3 = v^2 - (u^2 \partial v / \partial x + 2\Omega u) \Delta t \quad (3.6)$$

$$S^3 = S^2 - (w^2 \partial S / \partial z) \Delta t \quad (3.7)$$

Conditions (3.1) and (3.2) mean that u can be written in terms of a stream function ψ which vanishes on the boundaries. We seek a correction $\delta\psi$ to ψ which satisfies the equation

$$2\Omega \partial / \partial z [(\partial v / \partial x + 2\Omega) \delta\psi / \partial z] + (g e^{\sigma}) \partial / \partial x [(\partial \delta\psi / \partial x) (\partial S / \partial z)] = R / \Delta t^2 \quad (3.8)$$

where

$$R = (g e^{\sigma}) \partial S / \partial x - 2\Omega \partial v / \partial z.$$

This equation is elliptic provided $\partial S / \partial z$ and $\partial / \partial x (v + 2\Omega x)$ are both positive, as was assured in the adjustment procedure. If, instead, the whole of equations (3.4) and (3.5) were used to construct (3.8), extra cross-derivative terms would appear. The condition for ellipticity is then (2.30). It is found that this apparently more accurate procedure is highly unstable when the exact solution is discontinuous. The procedure using (3.8) is better conditioned and safer, though more iteration may be required.

After solving (3.8) for $\delta\psi$ using the boundary condition $\delta\psi = 0$, values δu and δw are generated from it and used to correct S and

v :

$$v^4 = v^2 - (\delta u \partial v / \partial x + \delta w \partial v / \partial z + 2\Omega \delta u) \Delta t \quad (3.9)$$

$$S^4 = S^2 - (\delta u \partial S / \partial x + \delta w \partial S / \partial z) \Delta t \quad (3.10)$$

v^4 and S^4 will not exactly satisfy (3.3) and so the correction step must be iterated. The final iteration can be combined with the predictor step for the next timestep, because equations (3.9) and (3.10) have the same form as equations (3.4) and (3.5).

3.2 Solution of the primitive hydrostatic equations

In this section we describe how equations (2.22)-(2.27) would normally be solved in the context of a weather prediction model. We relate the procedure closely to that set out above for the semi-geostrophic equations. It is usually assumed that the solution of the more general set of equations will automatically include those of the semi-geostrophic equations, as well as allowing other types of motion in the appropriate circumstances. In most operational models the only motions that can be resolved are hydrostatic. Thus we illustrate the solution of equations (2.22), (2.23), (2.25)-(2.27) and (2.29).

The problem will again be solved in a rectangular domain in the (x, z) plane. The equations can be made entirely explicit except for the constraint:

$$\int u \, dz = 0 \quad (3.11)$$

implied by (2.26) and (2.27). If an explicit time integration scheme is used, the size of the timestep is restricted by the usual Courant condition. The propagation speed that determines the maximum timestep is the highest phase speed of the waves described by the equations. Gadd (1978) introduced a splitting technique that means that only a few terms in the equations have to be computed with a short timestep. Many other ways of achieving this are described in the meteorological literature; we use a version of Gadd's technique here.

In a purely two-dimensional problem, the arrangement of variables on the grid could be the same as shown in Fig.3. However, in the three-dimensional problem with these equations there are no separate u_s and u variables. The continuity equation and boundary conditions again take the form (3.1) and (3.2). In a three dimensional problem the natural arrangement would be to hold u and v at different points—the C grid of Arakawa and Lamb(1977). This conflicts with the requirement that v and S be arranged to suit (3.3) and that the number of degrees of freedom in w matches the number of geostrophic constraints. It is therefore necessary to compromise. There is no general agreement as to which arrangement of variables is most suitable for the primitive hydrostatic equations.

The first stage of the forward time integration can be written:

$$v^1 = v^0 - (u \partial v / \partial x + 2\Omega u) \Delta t \quad (3.12)$$

$$S^1 = S^0 - (u \partial S / \partial x) \Delta t \quad (3.13)$$

The vertical advection of S is omitted at this stage because it forms part of the equation describing fast-moving gravity waves. It is therefore convenient to postpone calculation of the vertical advection of v . Any other forcing terms are included at this stage. In order to allow stable explicit forward time integration as suggested by (3.12) and (3.13), a two-step scheme such as the Heun or Lax-Wendroff is used.

Since there is no equation of the type (3.8) to solve, the adjustment procedure described in section 3.1 should not be necessary. However, it is found that very unrealistic flows develop if $\partial S / \partial z < 0$ because the real convective overturning that would take place in these circumstances cannot be described correctly by the hydrostatic

equations. It is therefore necessary to adjust the vertical profiles of S to ensure that $\partial S / \partial z > 0$. It is not considered necessary to perform horizontal adjustment or to attempt to enforce (2.30), though recent work e.g. Thorpe and Emanuel(1985) suggests that it may be advantageous. It is usual to combine this adjustment with a more sophisticated attempt to represent the effect of convective clouds on the atmosphere.

The third part of the solution is given by:

$$v^3 = v^2 - (w \partial v / \partial z) \Delta t \quad (3.14)$$

$$S^3 = S^2 - (w \partial S / \partial z) \Delta t \quad (3.15)$$

$$\partial \phi^3 / \partial z = g e^3 \quad (3.16)$$

$$u^3 = u^2 - (\partial \phi^3 / \partial x - 2\Omega v^3) \Delta t \quad (3.17)$$

$$\partial u^3 / \partial x + \partial w^3 / \partial z = 0 \quad (3.18)$$

The solution of (3.17) must be modified to enforce $\int u \, dz = 0$. The degree of freedom that allows this, is the unknown value of ϕ at $z=0$. (3.17) is first solved with $\phi=0$ at $z=0$. Let the resulting vertical mean of u^3 be U . The equation for the surface value ϕ_* of ϕ is then

$$\partial^2 \phi_* / \partial x^2 = \partial U / \partial x \quad (3.19)$$

with boundary conditions

$$\partial \phi_* / \partial x = 0 \text{ at } x=\pm L \quad (3.20)$$

This extra step is an artefact of our simplification of the equations to obtain (2.22)-(2.27). In operational forecast models, (3.19) is replaced by an explicit evolution equation for the surface pressure.

Equations (3.14) to (3.18) are solved using a shorter timestep than (3.12) and (3.13). They must thus be integrated several times for each integration of (3.12) and (3.13). This step plays the dual roles of acting as an explicit iterative solution of the implicit

equation (3.8) and providing explicit prediction of wave motions excluded by the semi-geostrophic system.

This description suggests a number of purely numerical problems that may arise in simulating a solution close to that of the semi-geostrophic equations by using a primitive equation model. It is not possible to define an arrangement of variables on the grid that is natural for the definition of geostrophic balance and is also suitable for the implicit calculation of the ageostrophic wind. If (3.14) to (3.18) are considered as an explicit iteration towards the solution of (3.8), the rate of convergence can be shown to be very slow unless the vertical scale of the motion is large, typically several km; Cullen and Norbury (1987). There is thus a risk that a primitive equation model could generate an unrealistically large amount of transient gravity and inertia wave motions.

4. NUMERICAL RESULTS

4.1 Front formation

In this section we compare results from finite difference solutions of the semi-geostrophic equations and the primitive hydrostatic equations in two two-dimensional test problems. The first problem is to simulate the evolution of a two-dimensional air-stream under the action of a large scale deformation field. The deformation rate is periodic in time so that a given cross-sectional area through the air-stream undergoes alternate compression and expansion. The data are chosen so that the semi-geostrophic solution forms a discontinuity which propagates into the interior of the fluid, as in the cases illustrated by Cullen and Purser (1984). As the deformation reverses, the discontinuity weakens and eventually the initial data is recovered. The total energy will be conserved over the cycle. As discussed in section 2, this solution represents the minimum energy state that can be reached by the two-dimensional primitive equations without mixing. Thus, when solving this problem using finite difference approximations to either the semi-geostrophic or to the primitive hydrostatic equations, the same solution should be obtained up till the formation of a discontinuity—provided that total energy is conserved by the finite difference schemes. After this point, smoothing has to be used to allow the integration to be continued. When the expansion phase begins, some of the parcel properties which determine the minimum energy configuration may have been modified. It is therefore not likely that the original solution will be recovered at the end of the cycle, the error will reflect the amount of smoothing needed in the integration. The final solution will contain less energy than the original and in the solution

of the primitive equations some of the energy lost from the basic state may appear as inertia-gravity waves.

The semi-geostrophic equations for this problem are :

$$\partial \phi / \partial x = 2\Omega v \quad (4.1)$$

$$\partial \phi / \partial z = g e^{\sigma} \quad (4.2)$$

$$DM/Dt = -\sigma M \quad (4.3)$$

$$DS/Dt = 0 \quad (4.4)$$

$$DA/Dt = -\sigma A \quad (4.5)$$

$$u = \bar{u} + \sigma x \text{ at } x = \pm L \int e^{-\sigma r} dr \quad (4.6)$$

The deformation rate σ is proportional to $\cos(\omega t)$. The primitive hydrostatic equations are obtained by adding Du/Dt to the left hand side of (4.1).

If this situation arose in a normal forecast model it would not be practicable to adjust the grid with the deformation. The results illustrated therefore use a fixed grid and always integrate between $x=\pm L$. Extra boundary conditions, that $Me^{\sigma t}$ and S are fixed at $x=\pm L$ during the compression phase, have to be specified.

Results from the semi-geostrophic integration are shown in Fig. 4. The deformation was chosen so that the maximum compression of the original cross-section was 28%. The equations were solved on a uniform 50×12 grid. The results, however, are shown only for the region bounded by $x = \pm L \int e^{-\sigma r} dr$. The entropy field is illustrated at the maximum compression and expansion during the first and fifth cycles. The results near the front are almost identical on the two cycles. There are

slight differences near the boundaries because of the use of extra boundary conditions.

Results from the primitive hydrostatic equations are shown in Fig. 5. After the initial compression the entropy field is very similar to the semi-geostrophic model. However, the cross-frontal circulation does not fall to near zero as the deformation rate drops to zero at the maximum compression, but remains near its maximum value. In the expansion phase the circulation changes sign as in the semi-geostrophic model but overshoots the value reached during compression. The expansion phase, therefore, leads to a much greater spreading out of the entropy gradient. By the fifth cycle the compression gives almost vertical isentropes, while the expansion spreads the entropy gradient over the whole domain.

The difference between these solutions can be explained by their different responses to a time-varying deformation. The semi-geostrophic model produces a cross-frontal circulation determined by the instantaneous deformation rate. The primitive equation model circulation is predicted as an initial-value problem. Linear theory, as described Haltiner and Williams (1980), shows that the solution will only be similar to that of the semi-geostrophic model if the time-scale of the variation in the deformation is much greater than f^{-1} . In the solutions shown here the time-scales were intentionally made comparable to highlight the difference. It is very hard to determine from observations whether the real ageostrophic circulation responds on the time-scale given by linear theory, or whether nonlinear or turbulent motions damp the non-equilibrium part of the ageostrophic circulation leading to faster adjustment.

4.2 Mountain flow

The second problem to which we compare solutions is that of two-dimensional flow over a mountain ridge. The basic flow is in geostrophic balance with a pressure gradient parallel to the ridge. This pressure gradient is maintained at a constant value and provides the source of energy for the problem. The ridge is chosen to be a typical Alpine cross-section. The problem is restrictive as a model of the real atmosphere because all the air has to flow across the ridge. In many real situations a large proportion flows round the mountains and does not undergo significant vertical displacement. The problem has been discussed in detail by Cullen, Chynoweth and Purser (1987). They show that the semi-geostrophic solution concentrates the flow across the ridge into a shallow jet, with little disturbance to the air higher up. A strong flow develops along the upwind slope of the ridge, which would in a three-dimensional calculation take air round the end of the ridge without vertical displacement. This solution again represents the minimum energy state that can be reached in two-dimensional flow subject to parcel conservation properties and the requirement that no fluid can flow through the ridge. Total energy decreases in this problem; it is extracted from the assumed basic state pressure gradient and is dissipated when air descends on the lee side. The rate of loss of energy equals the drag on the mountain multiplied by the speed of the basic flow.

When solving the semi-geostrophic equations the energy dissipation is implicit and is assumed to be achieved by motions not described by the equations. The numerical method must be able to deal with this. A solution of the primitive hydrostatic equations can release

the energy in unbalanced wave motions; or dissipate the energy by sub-grid scale eddy diffusion terms, or by the vertical adjustment which maintains $\partial S / \partial z \geq 0$ - the condition for gravitational stability. It is not known under what circumstances which process is dominant.

The semi-geostrophic equations to be solved in this case are:

$$\partial \phi / \partial x = 2\Omega v \quad (4.7)$$

$$\partial \phi / \partial z = g e^{\sigma} \quad (4.8)$$

$$DM/Dt = 2\Omega U \quad (4.9)$$

$$DS/Dt = 0 \quad (4.10)$$

$$DA/Dt = 0 \quad (4.11)$$

$$u = U \text{ at } x = \pm L \quad (4.12)$$

The primitive hydrostatic equations are obtained by adding Du/Dt to (4.7). The initial data is shown in Fig. 6. The ridge is 2000m high and 250km wide. The total length of the integration domain is 1300km. There is a front crossing the ridge with a strong jet of 32ms^{-1} parallel to the ridge. Because of (4.7) and (4.8), this is associated with a slope in the isentropes (S contours) in the middle of the atmosphere. The irregularities at upper levels over the ridge are caused by interpolation from the terrain-following coordinates used in the computations to physical height as an output coordinate.

The semi-geostrophic solution is shown in Fig. 7. The equations were solved on a uniform 40×10 grid. The results are after a 12 hour time interval with a basic cross-mountain wind U of 15ms^{-1} . The S field, Fig. 7(a) shows that the frontal zone has not been distorted by

its passage over the ridge but the slope has been reduced. Most of the enhanced flow across the ridge is confined to the lowest model layers. Fig. 7(b) shows the wind parallel to the ridge. The upper air maximum has been reduced to 25ms^{-1} . There is an upstream barrier jet at low levels of 12ms^{-1} ; downstream there is a region of uniform negative v of about 5ms^{-1} . This results from the bulk displacement of air to the right of the position it would have occupied in the absence of the ridge. Since M is determined as a function of t by (4.9) for each parcel of air, an increase in x must be compensated by a decrease in v .

The implied cross-ridge circulation (u, w) is shown in Figs. 7(c) and (d). The perturbation to u is less than 1ms^{-1} almost everywhere except near the ridge top. The maximum value is there about 65ms^{-1} . Upstream of the ridge the basic 15ms^{-1} is reduced to less than 8ms^{-1} . The vertical motion is mainly confined to the vicinity of the ridge. A narrow tongue of values up to 13cms^{-1} extends up to the top of the model above the ridge; this is almost certainly caused by numerical errors.

The solution of the primitive hydrostatic equations is shown in Fig. 8. The entropy field shows a large amplitude hydraulic-type flow over the ridge with a downstream jump. Overturning of the isentropes there is prevented by the vertical adjustment procedure. There is a standing wave over the mountain top at upper levels. The downstream cold air retains its identity in a cold 'dome'. The wind component along the ridge is shown in Fig. 8(b). The main jet is reduced in amplitude by a similar amount to the semi-geostrophic model. However, other changes are much larger. The upstream barrier jet reaches 20ms^{-1} and is deeper than in the semi-geostrophic model. There are large

negative values generated above the ridge top where the hydraulic flow is dragging air down and to the right across the ridge. There is an extra region of positive values below the main jet, where the air downstream is swept back towards the ridge in a type of rotor motion. The horizontal cross-ridge wind, Fig. 8(c) shows the hydraulic flow and the downstream rotor. There is a region of retarded flow upstream similar to the semi-geostrophic model. The vertical motion, Fig. 8(d), shows the motions discussed above, together with some wave motions propagating away from the ridge.

These two calculations have produced very different solutions. The adjustment step in the semi-geostrophic solution which enforces monotonicity of $(v+2\Omega x)$ is used at most time-steps and, together with the removal of small scales from the (u, w) field used to provide a first guess at the next time-step, allows the energy to be removed quite effectively. However, there are noticeable errors in the solution above the ridge, indicating that the scheme has not removed all that is required to reach the minimum energy configuration. In the primitive equation integration, much of the energy appears in the hydraulic flow and is dissipated in the downstream jump through the vertical adjustment procedure. A similar mechanism is implied in the semi-geostrophic model when fluid 'jumps' over the ridge. However, the primitive equation solution drags air down to near the surface from well above the ridge, while the semi-geostrophic disturbance would only reach a short distance above it. This is because the primitive equation solution has to represent the response on resolved scales up till the point when the jump 'breaks' - the point when three-dimensional and non-hydrostatic motions would be generated.

5. DISCUSSION

The integrations shown illustrate the difficulty of maintaining balanced flow in a numerical integration under conditions where the balanced solution is not smooth, or when the forcing varies on a time-scale comparable to f^{-1} . In the case of time-varying forcing, it is not known whether the atmosphere remains close to balance only if the time-scale is an order of magnitude greater than f^{-1} , as would be required by linear theory, or whether nonlinear effects allow balance with more rapidly varying forcing. When the balanced solution is not smooth, there will be at least a local breakdown of balance in the atmosphere. However, the strong gradients mean that the real flow will not remain two-dimensional either. In the solutions of the primitive hydrostatic equations illustrated, the response has to be on scales resolved by the model and has to be smooth and two-dimensional. These restrictions exclude the balanced solution, which is not smooth, and prevent realistic modelling of the unbalanced flow.

The real problem which has to be solved in numerical weather prediction is three-dimensional and many of the perturbing mechanisms, such as the mountains are not well resolved. In the case of flow over a ridge for instance, the balanced response is primarily dependent on the maximum height and the area of the cross-section. The unbalanced response is also very dependent on the shape. The results shown in this paper illustrate that there is a serious question as to whether it is sensible to attempt explicit prediction of the unbalanced flow, or whether it is better to concentrate on accurate prediction of balanced flow.

ACKNOWLEDGEMENTS

The authors wish to thank Dr. J. Norbury for advice concerning the content of this paper, and Mr. M. W. Holt, Mr. M. Hatton and Mr. C. A. Parrett for programming assistance.

REFERENCES

- Arakawa, A. and Lamb, V. R. 1977 'Computational design of the basic dynamical processes of the UCLA general circulation model', Methods of Computational Physics, Vol. 17, Academic Press, 174-265, 337pp.
- Browning, G. L. and Kreiss, H. O. 1986 'Scaling and computation of smooth atmospheric motions', Tellus, 38A, 295-313.
- Cullen, M. J. P. 1987 'Implicit finite difference approximations to discontinuous atmospheric flows', U.K. Met. Office, Met. O 11 Tech. Note no. .
- Cullen, M. J. P. and Purser, R. J. 1984 'An extended Lagrangian model of semi-geostrophic frontogenesis', J. Atmos. Sci., 41, 1477-1497.
- Cullen, M. J. P., Chynoweth, S. and Purser, R. J. 1987 'On semi-geostrophic flow over synoptic scale topography', Quart. J. Roy. Meteor. Soc., 113, 163-180.
- Cullen, M. J. P., Norbury, J., Purser, R. J. and Shutts, G. J. 1987 'Modelling the quasi-equilibrium dynamics of the atmosphere', Quart. J. Roy. Meteor. Soc., 113, July issue.

Gent, P.R. and McWilliams, J.C. 1983 'Consistent balanced models in bounded and periodic domains', Dyn. Atmos. Oceans, 7, 67-93.

Gadd, A.J. 1978 'A split-explicit integration scheme for numerical weather prediction', Quart. J. Roy. Meteor. Soc., 104, 569-582.

Gadd, A.J. 1985 'The 15-level weather prediction model', Meteorol. Mag., 114, 222-226.

Haltiner, G.J. and Williams, R.T. 1980 'Numerical prediction and dynamic meteorology', John Wiley and Sons, 477pp.

Holt, M.W. 1987 'Moist frontogenesis in the geometric model', U.K. Met. Office, Met.O 11 Tech. Note no. 248.

Hoskins, B.J. 1975 'The geostrophic momentum approximation and the semi-geostrophic equations', J. Atmos. Sci., 32, 233-242.

Lorenz, E.N. 1969 'The predictability of a flow which possesses many scales of motion', Tellus, 21, 289-307.

Lorenz, E.N. 1984 'Prospects for improved weather forecasting', in proceedings of seminar on progress in numerical modelling, Sigtuna, Sweden, W.M.O., G.A.R.P. special report no. 43, pp. III 1-11.

Lilly, D.K. 1982 'Mesoscale variability of the atmosphere' in 'Mesoscale Meteorology: Theories, Observations and models', ed. D.K. Lilly and T. Gal-Chen, NATO ASI Series C no. 114, pp. 13-74.

Majda, A. 1986 'Vorticity and the mathematical theory of incompressible fluid flow', Comm. Pure Appl. Math., 39, S187-S220.

Pielke, R.A. 1984 'Mesoscale meteorological modelling', Academic Press, 612 pp.

Salmon, R. 1985 'New equations for nearly geostrophic flow', J. Fluid Mech., 153, 461-477.

Salmon, R. 1987 'Hamiltonian fluid mechanics', Ann. Rev. Fluid Mech., submitted.

Shutts, G.J. 1987 'A Hamiltonian formulation of semi-geostrophic theory for planetary scale flow', in preparation.

Shutts, G.J. and Cullen, M.J.P. 'Parcel stability and its relation to semi-geostrophic theory', J. Atmos. Sci., 44, April issue.

Temam, R. 1977 'Navier-Stokes equations', North-Holland, 500 pp.

Temperton, C. and Williamson, D.L. 1981 'Normal mode initialisation for a multi-level grid point model', Mon. weather Review, 109, 729-743.

Thorpe, A.J. and Emanuel, K.A. 1985 'Frontogenesis in the presence of small stability to moist slantwise convection', J. Atmos. Sci., 42, 1809-1824.

W.M.O. 1986 Extended abstracts of papers presented at the WMO/IUGG symposium on short and medium-range numerical weather prediction, W.M.O. Tech. Document no. 114.

LIST OF FIGURES

- Figure 1. Initial cross-section of fluid elements.
- Figure 2. Cross-section of fluid elements after deformation.
- Figure 3. Arrangement of variables on grid for semi-geostrophic solutions.
- Figure 4. Solutions for front formation under action of time-periodic deformation field, cross-sections of entropy, semi-geostrophic model:
- (a) maximum compression, 1st cycle.
 - (b) maximum expansion, 1st cycle.
 - (c) maximum compression, 5th cycle.
 - (d) maximum expansion, 5th cycle.
- Figure 5. Solutions for front formation using primitive equation model, details as Fig. 4.
- Figure 6. Initial data for flow over mountain:
- (a) Entropy cross-section.
 - (b) Geostrophic wind parallel to ridge (ms^{-1}).
- Figure 7. Solution for flow over mountain after 12 hours, semi-geostrophic model:
- (a) Entropy.
 - (b) Wind parallel to ridge (ms^{-1}).
 - (c) Horizontal wind across ridge (ms^{-1}).
 - (d) Vertical wind (cms^{-1}).
- Figure 8. Solution for flow over mountain, primitive equation model, details as Fig. 7.

LIST OF FIGURES

Figure 1. Cross-section of fluid elements after deformation.

Figure 2. Cross-section of fluid elements after deformation.

Figure 3. Cross-section of fluid elements after deformation.

Figure 4. Cross-section of fluid elements after deformation.

Figure 5. Cross-section of fluid elements after deformation.

Figure 6. Cross-section of fluid elements after deformation.

Figure 7. Cross-section of fluid elements after deformation.

Figure 8. Cross-section of fluid elements after deformation.

- geostrophic model:
- (a) maximum compression, 1st cycle.
 - (b) maximum expansion, 1st cycle.
 - (c) maximum compression, 2nd cycle.
 - (d) maximum expansion, 2nd cycle.

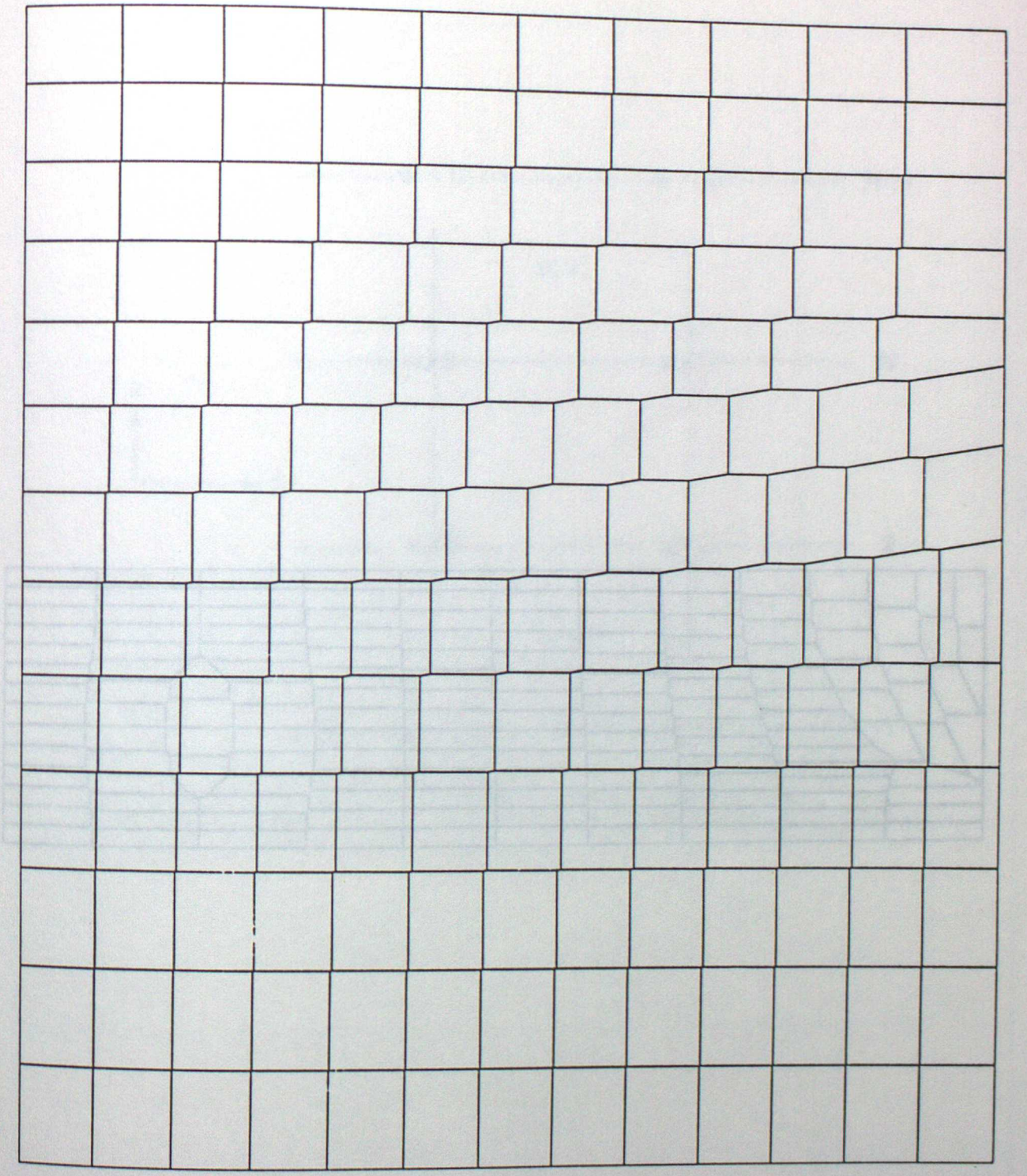
Figure 2. Solutions for flow formation over mountainous terrain, details as Fig. 1.

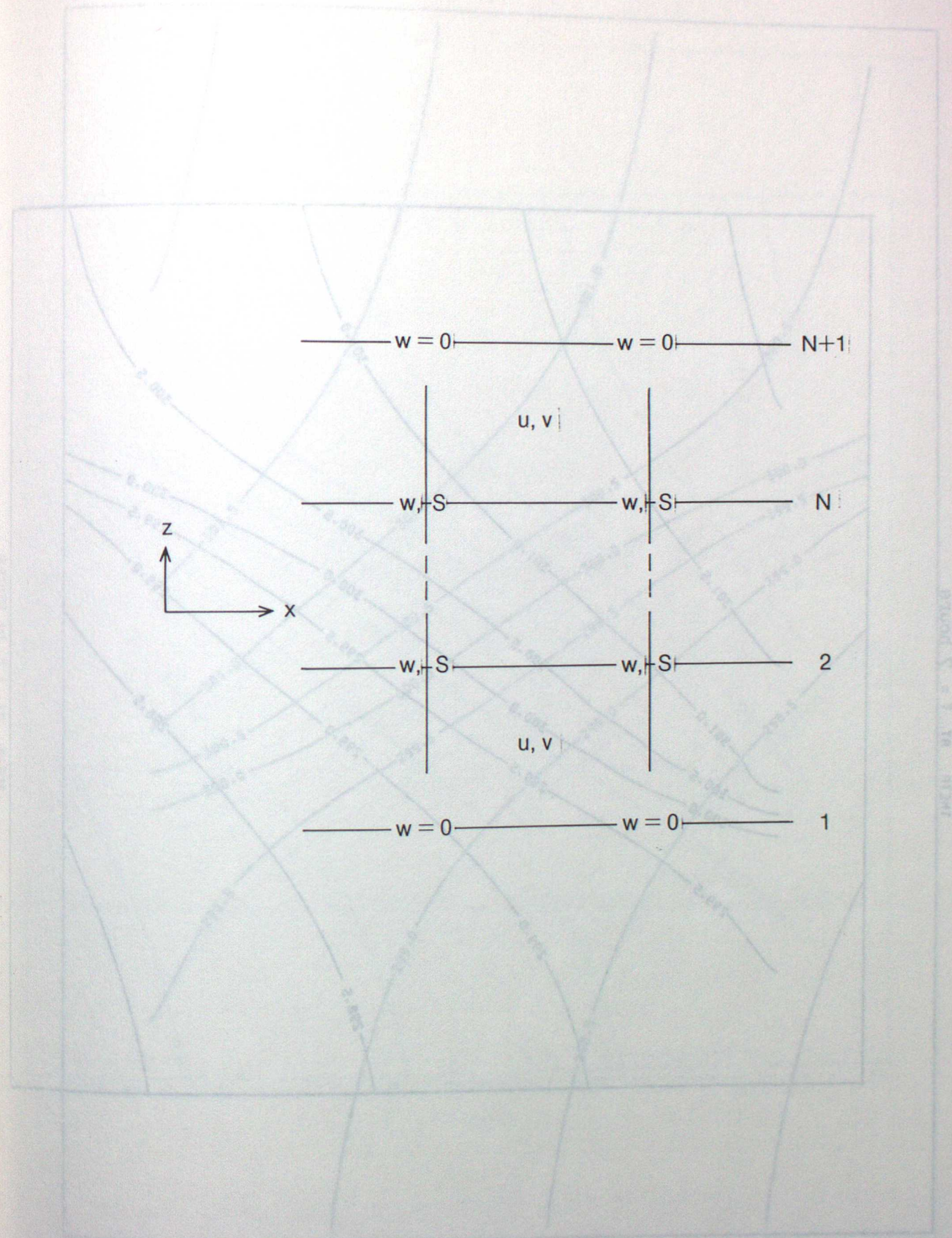
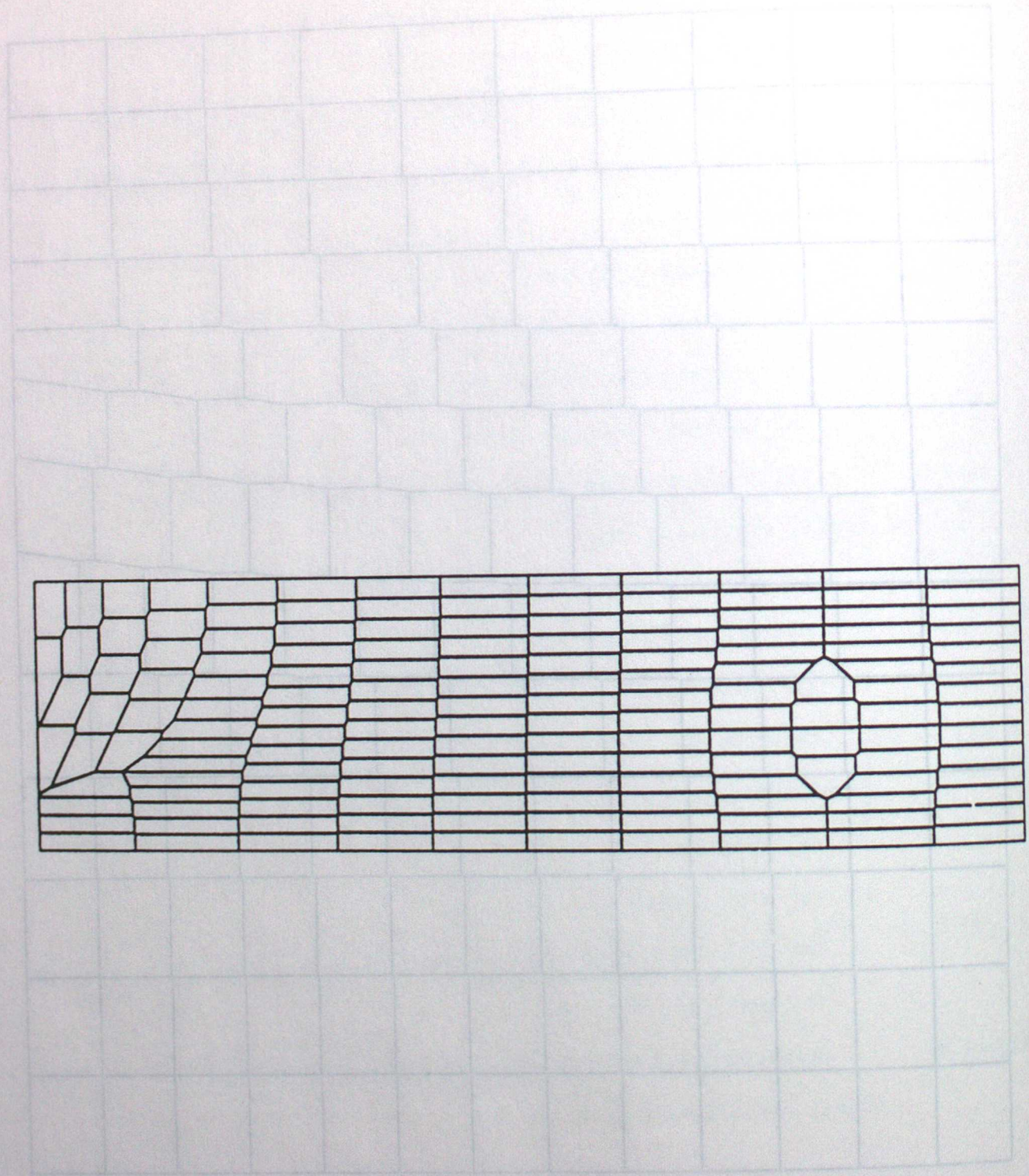
- Figure 3. Initial data for flow over mountainous terrain.
- (a) Energy cross-section.
 - (b) Geostrophic wind parallel to ridge.

Figure 4. Solution for flow over mountainous terrain, geostrophic model:

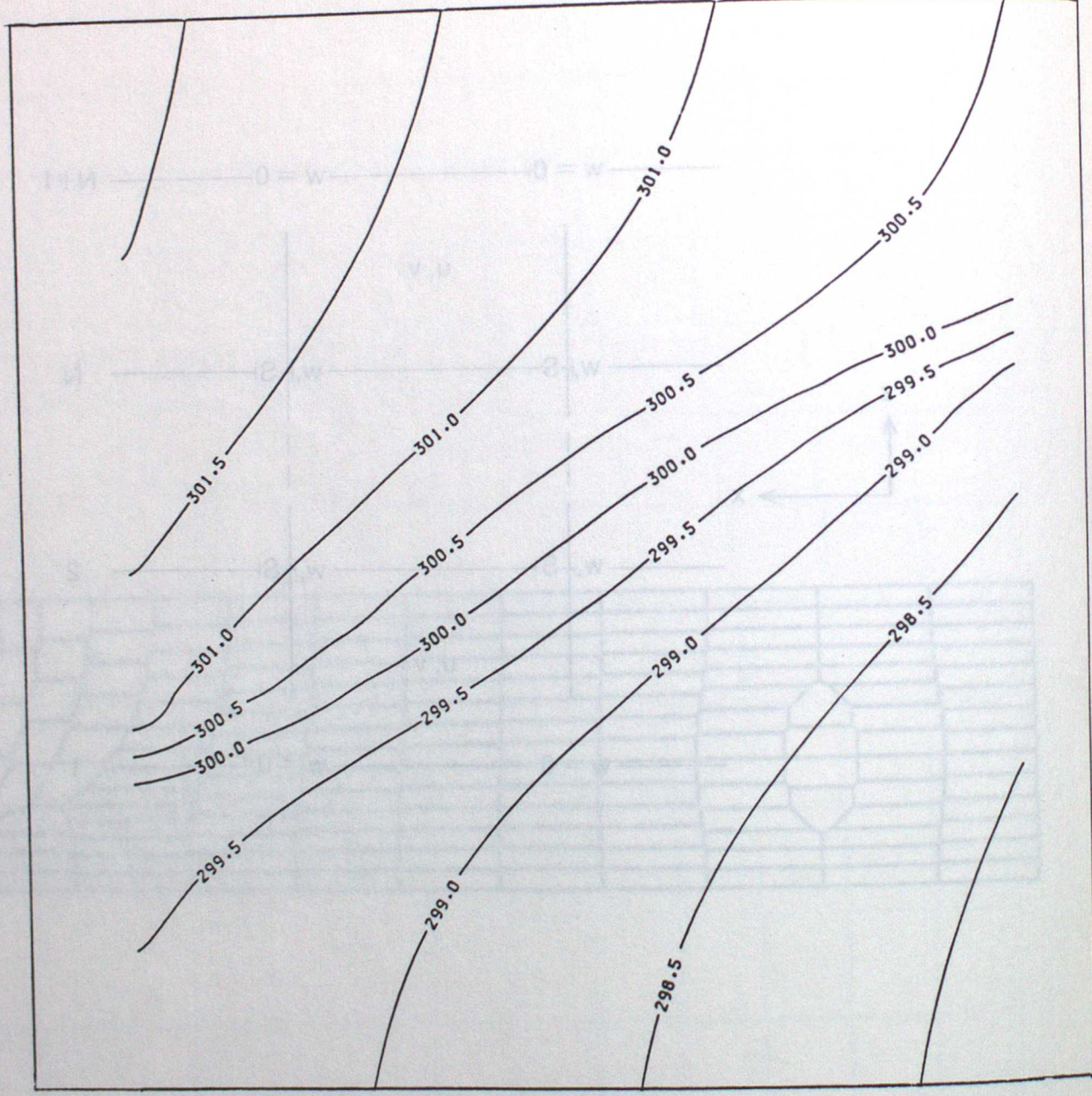
- (a) Energy.
- (b) Wind parallel to ridge.
- (c) Horizontal wind across ridge.
- (d) Vertical wind.

Figure 5. Solution for flow over mountainous terrain, primitive equation model, details as Fig. 4.

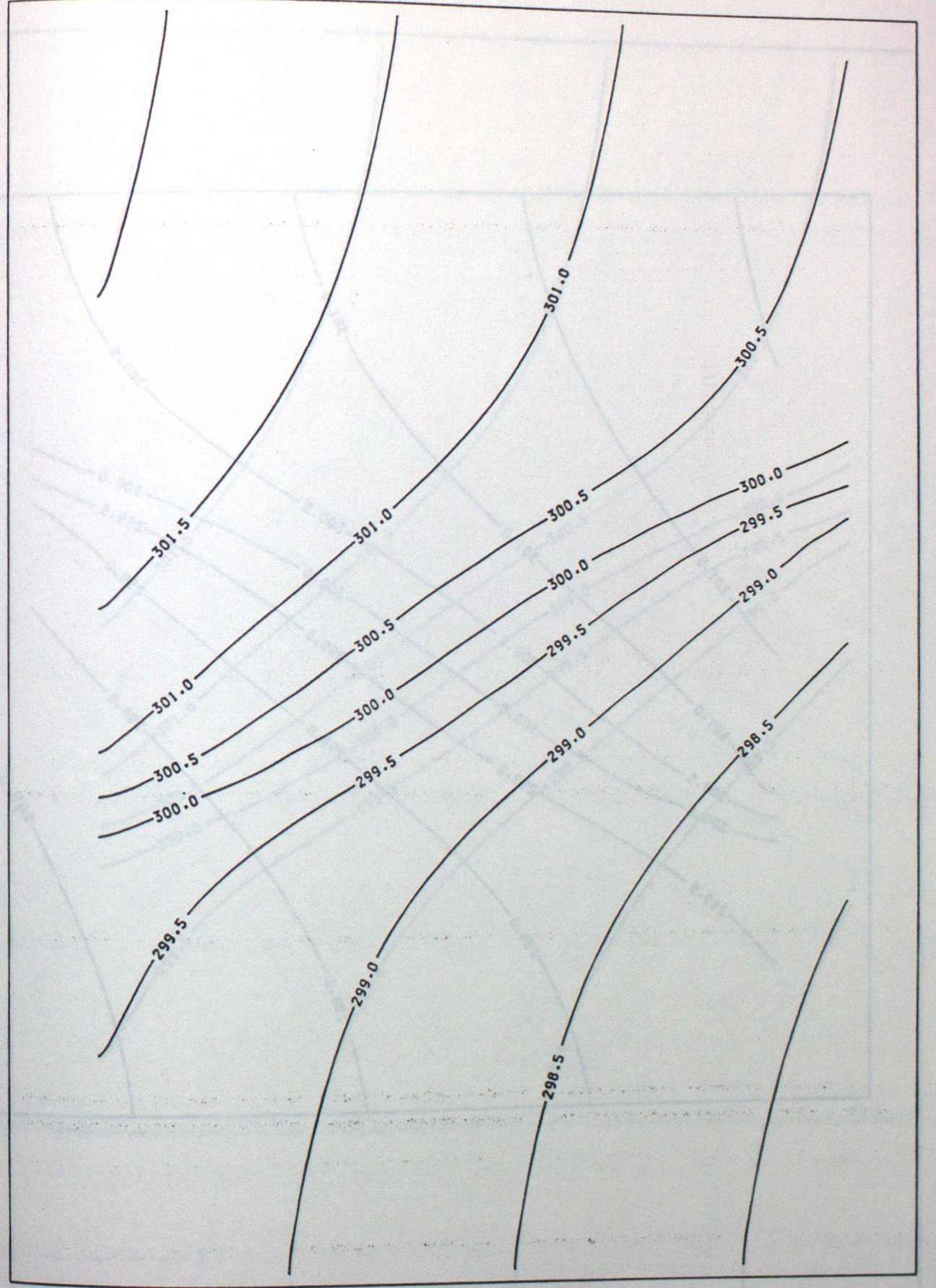




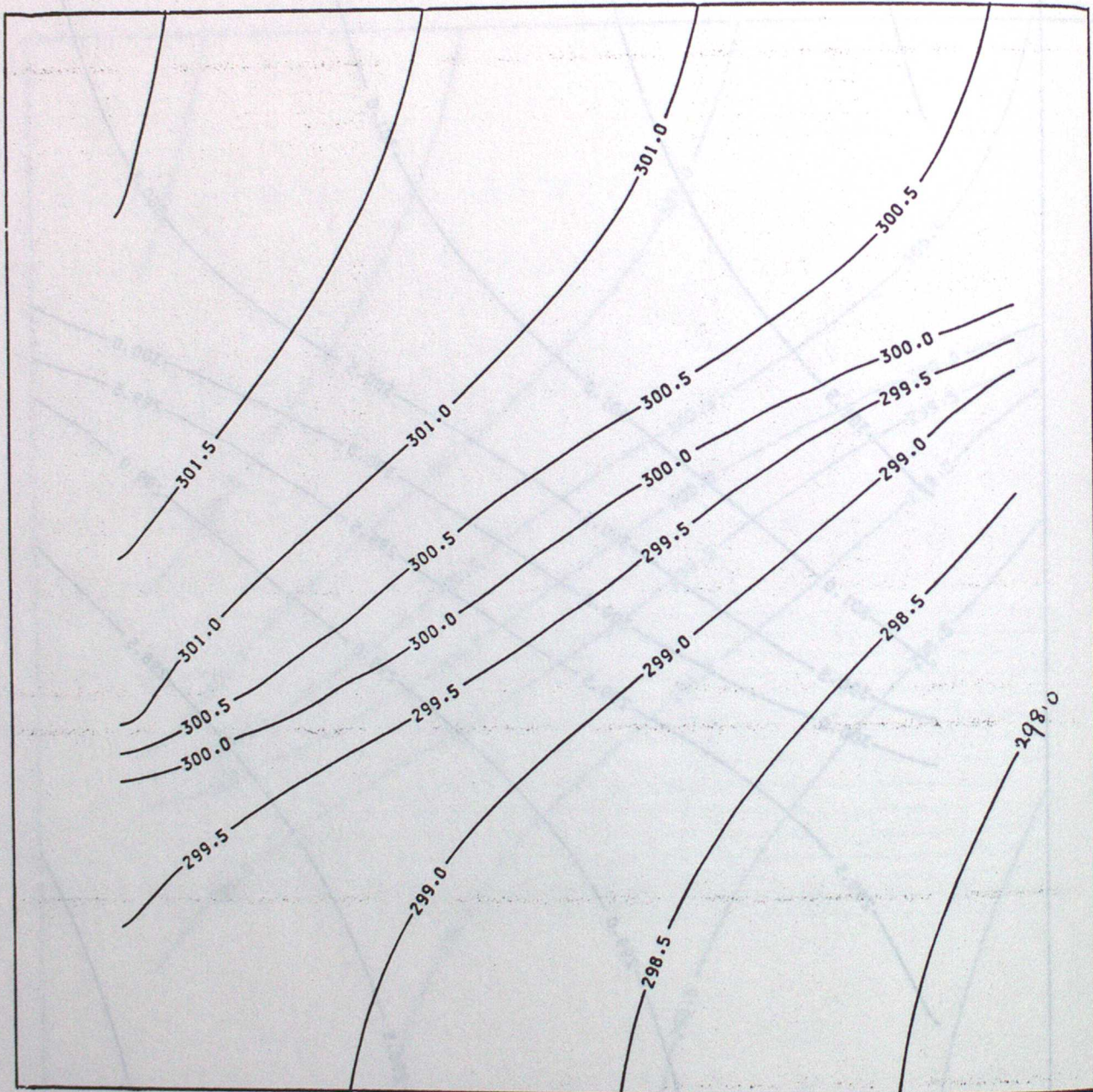
THETA AT T = 7 hours



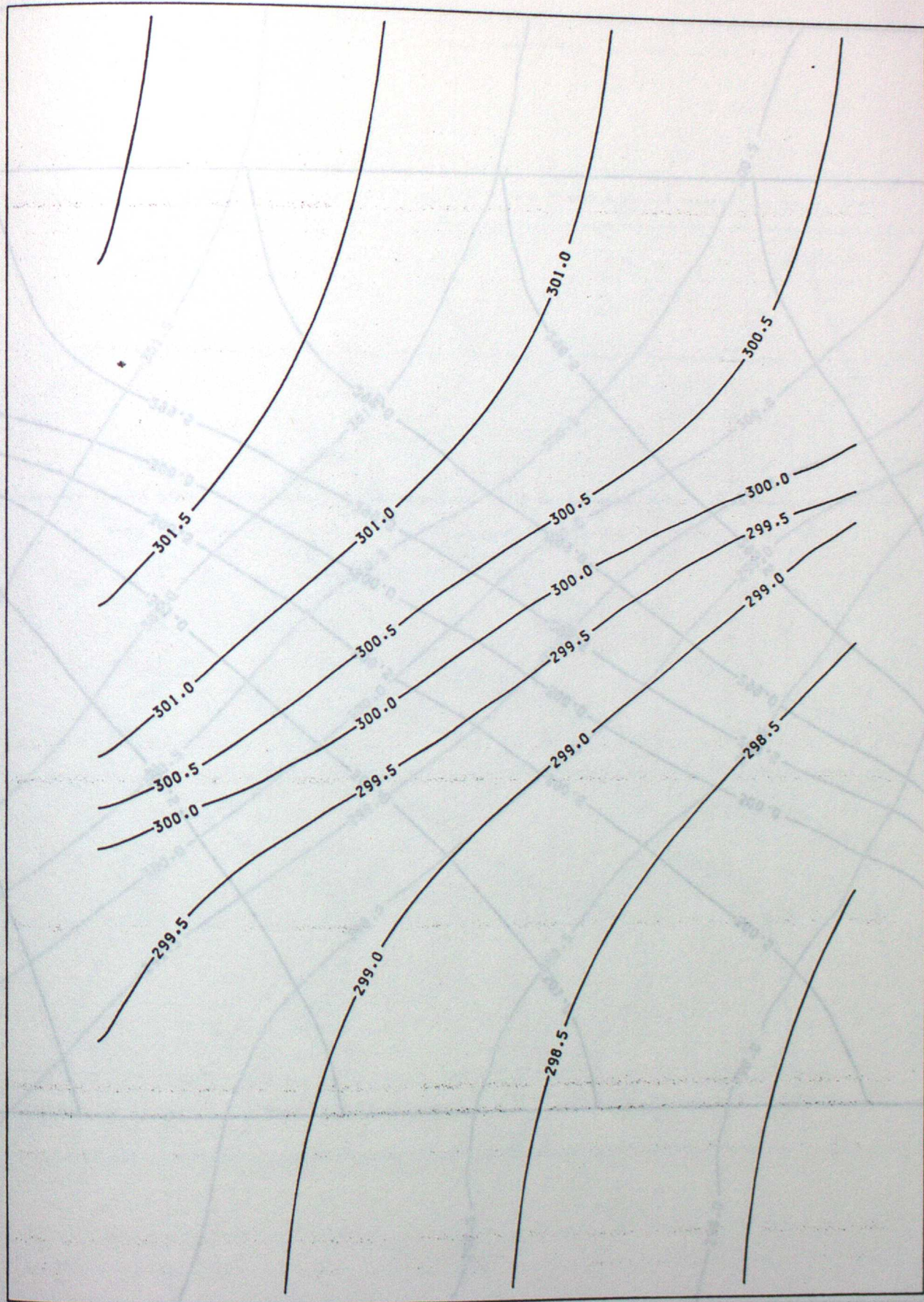
THETA AT T = 14 hours

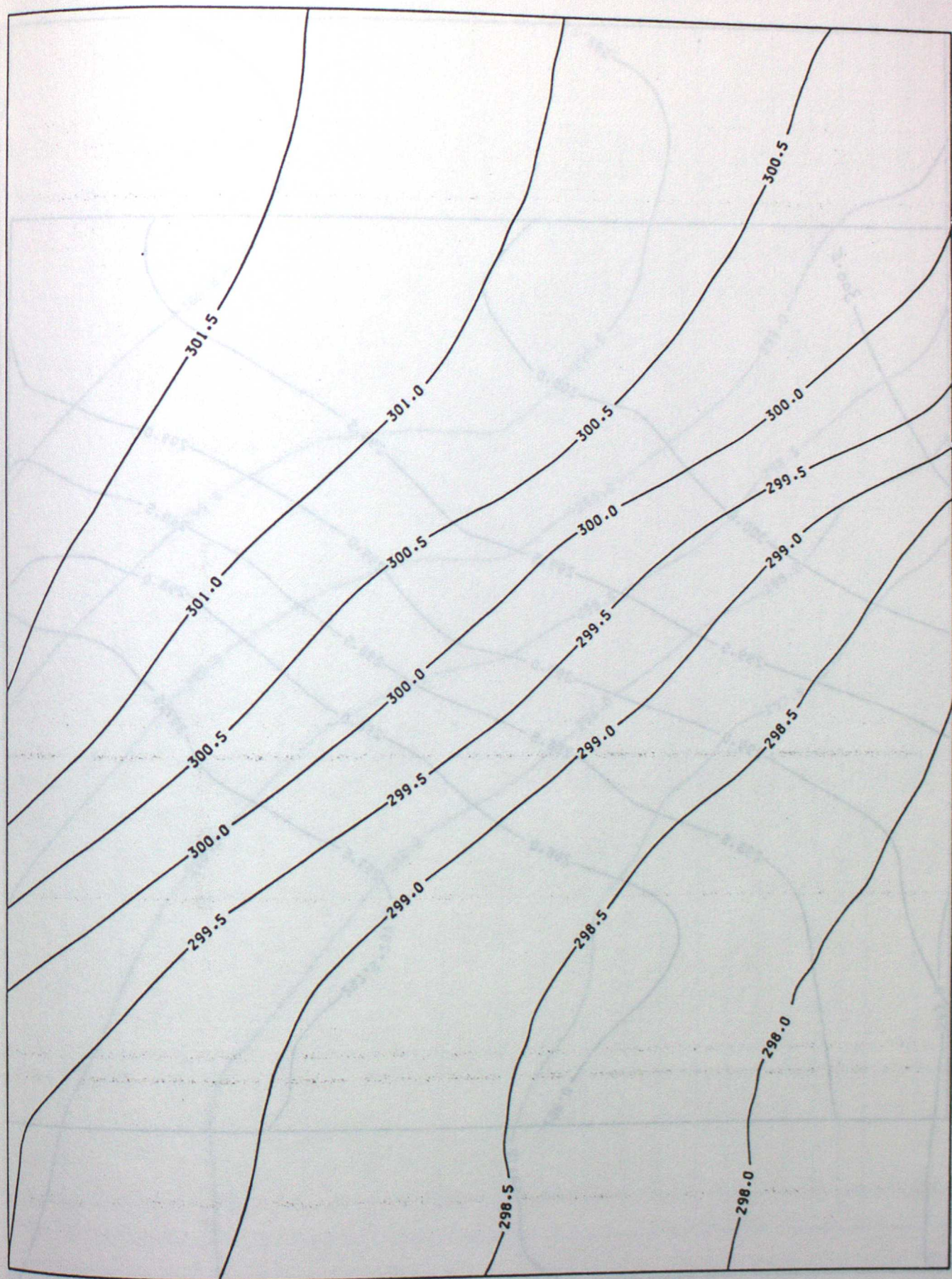
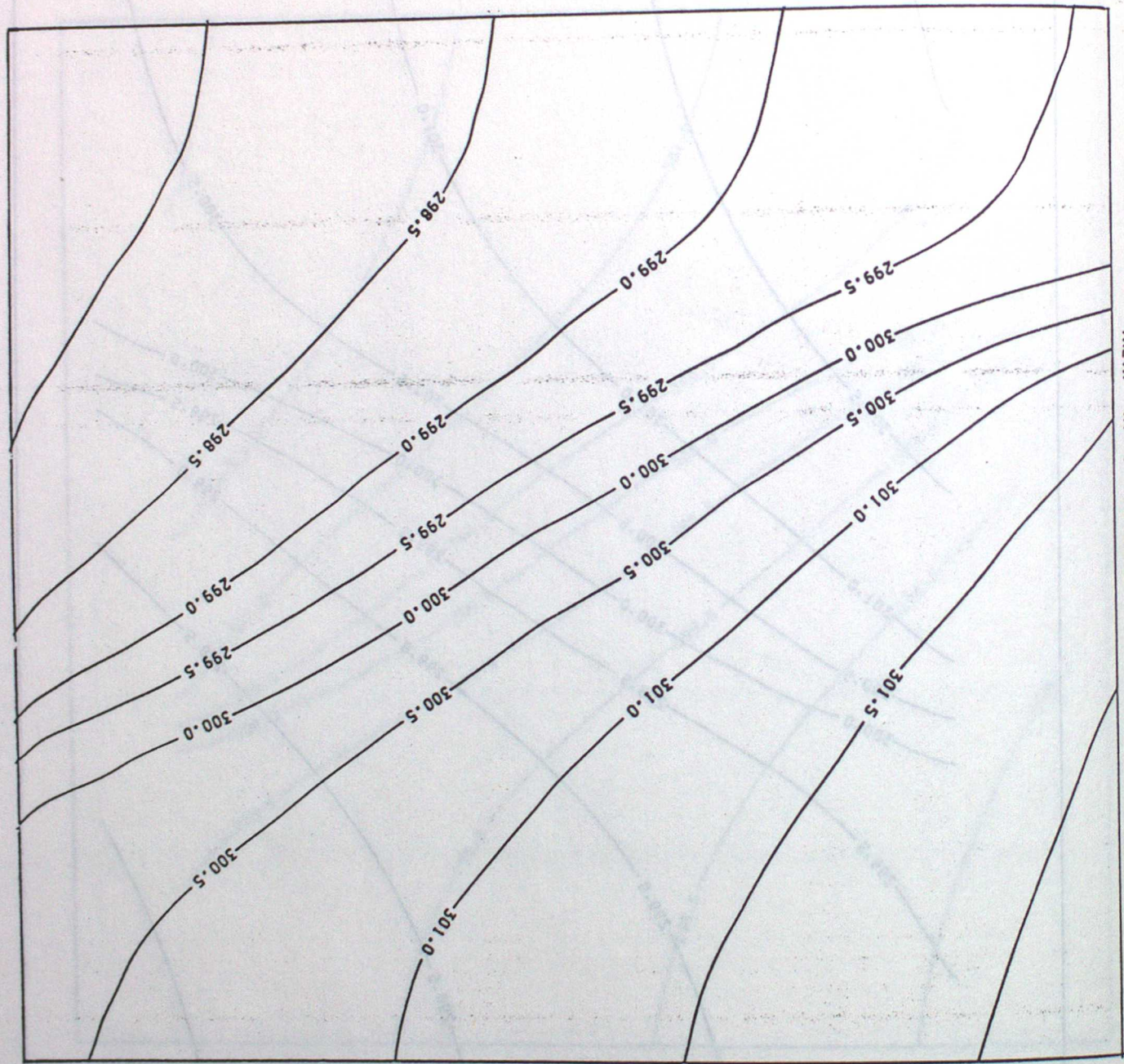


THETA AT T = 62 hours

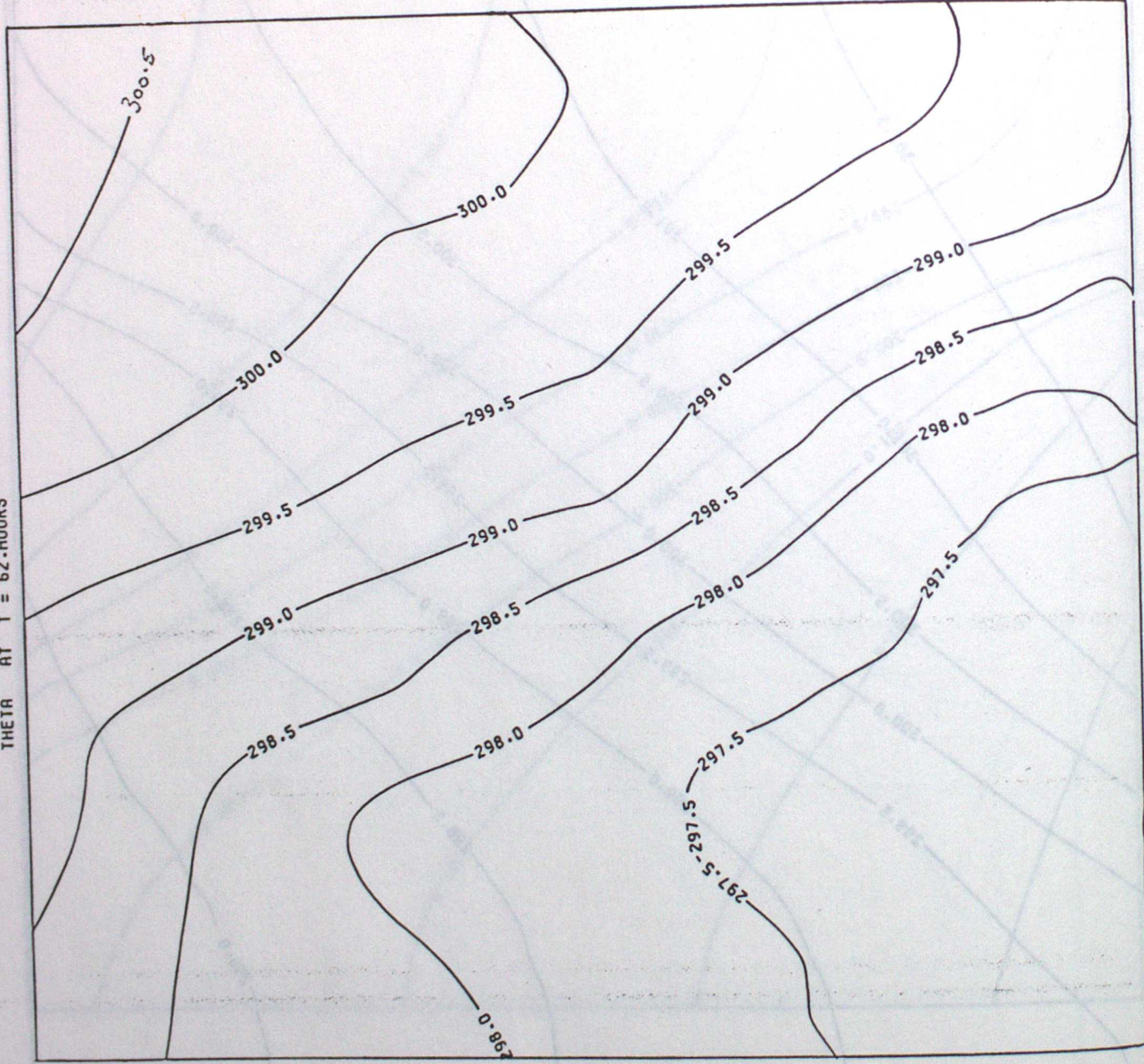


THETA AT T = 69 hours

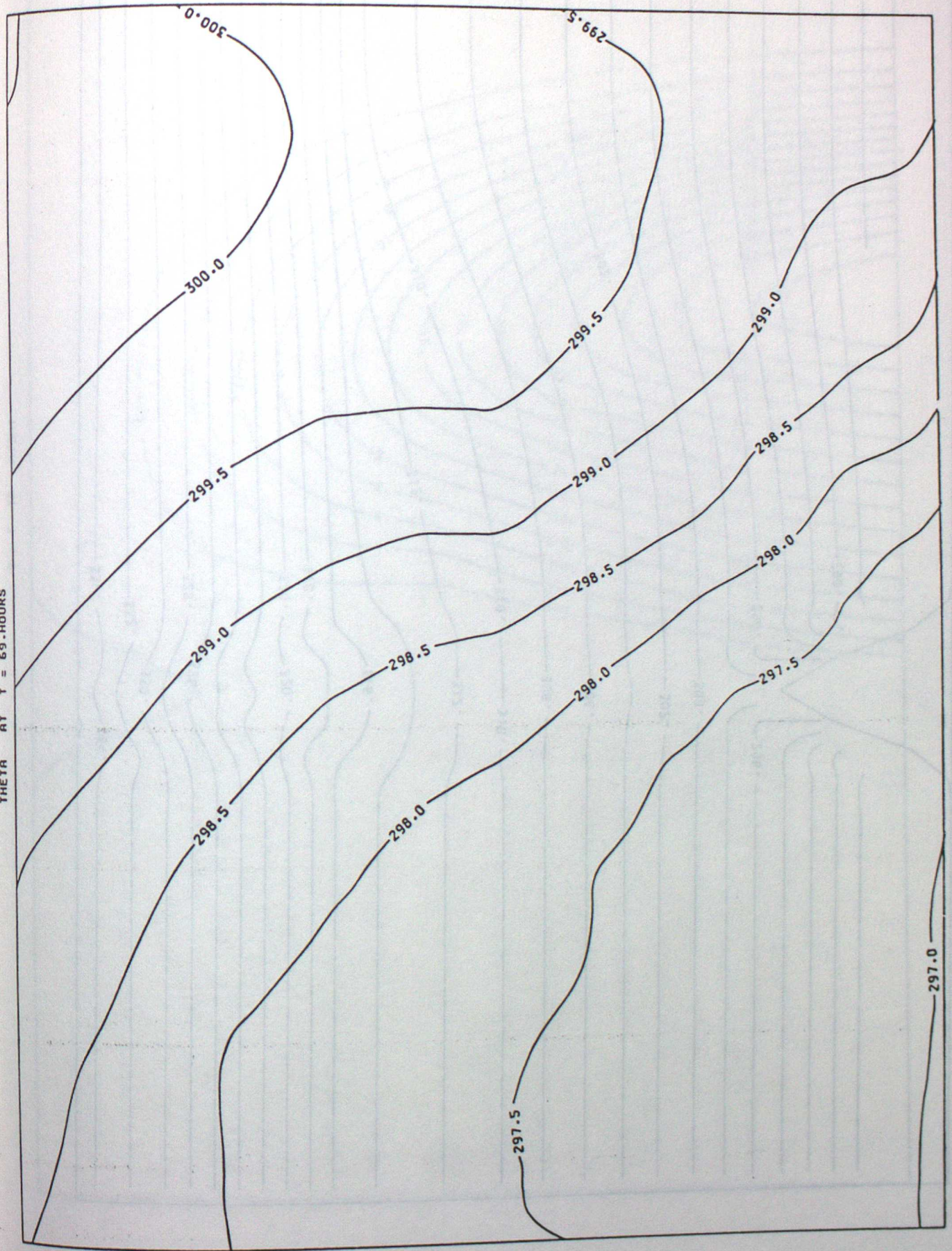




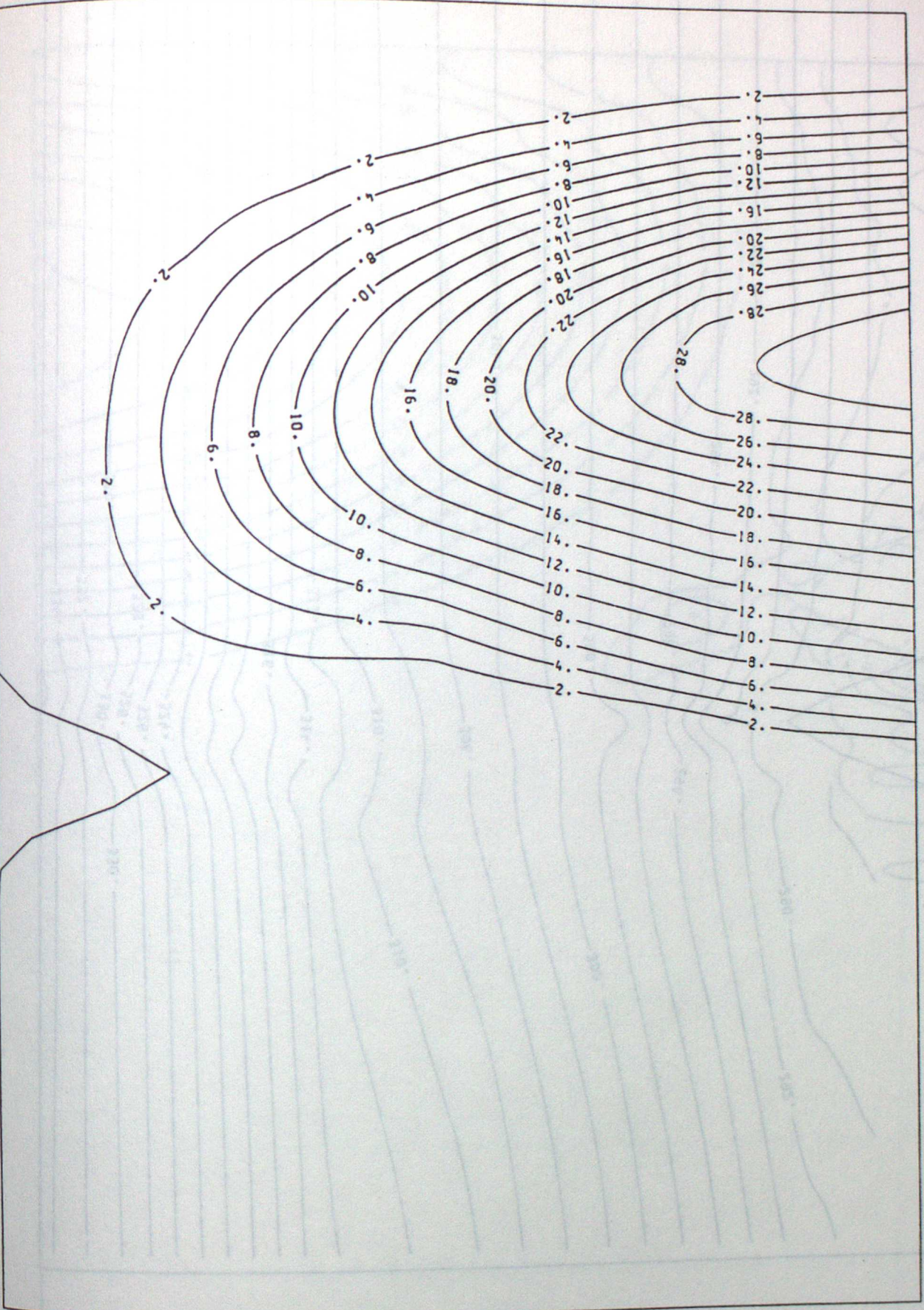
THETA AT T = 62 HOURS



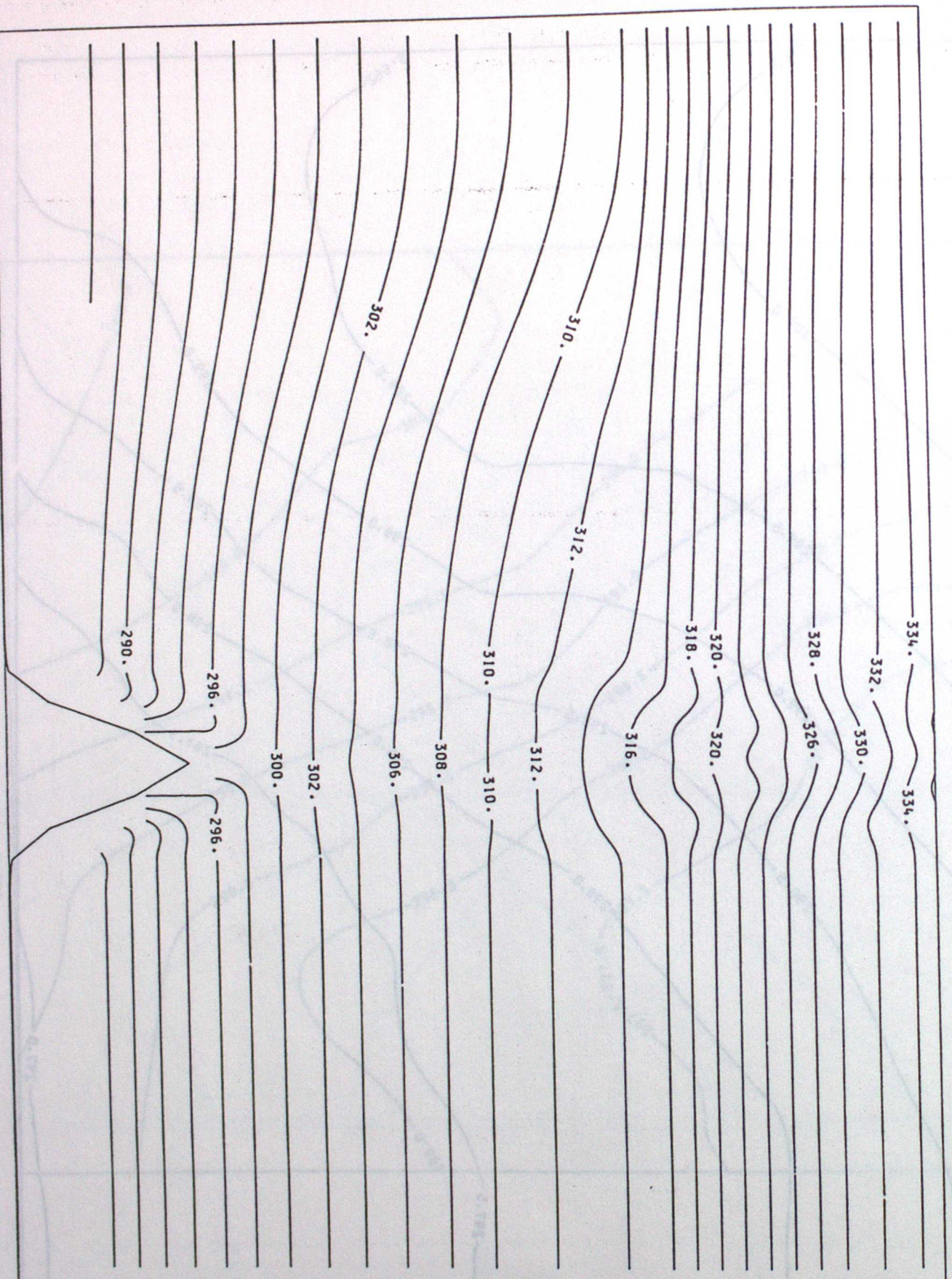
THETA AT T = 69 HOURS

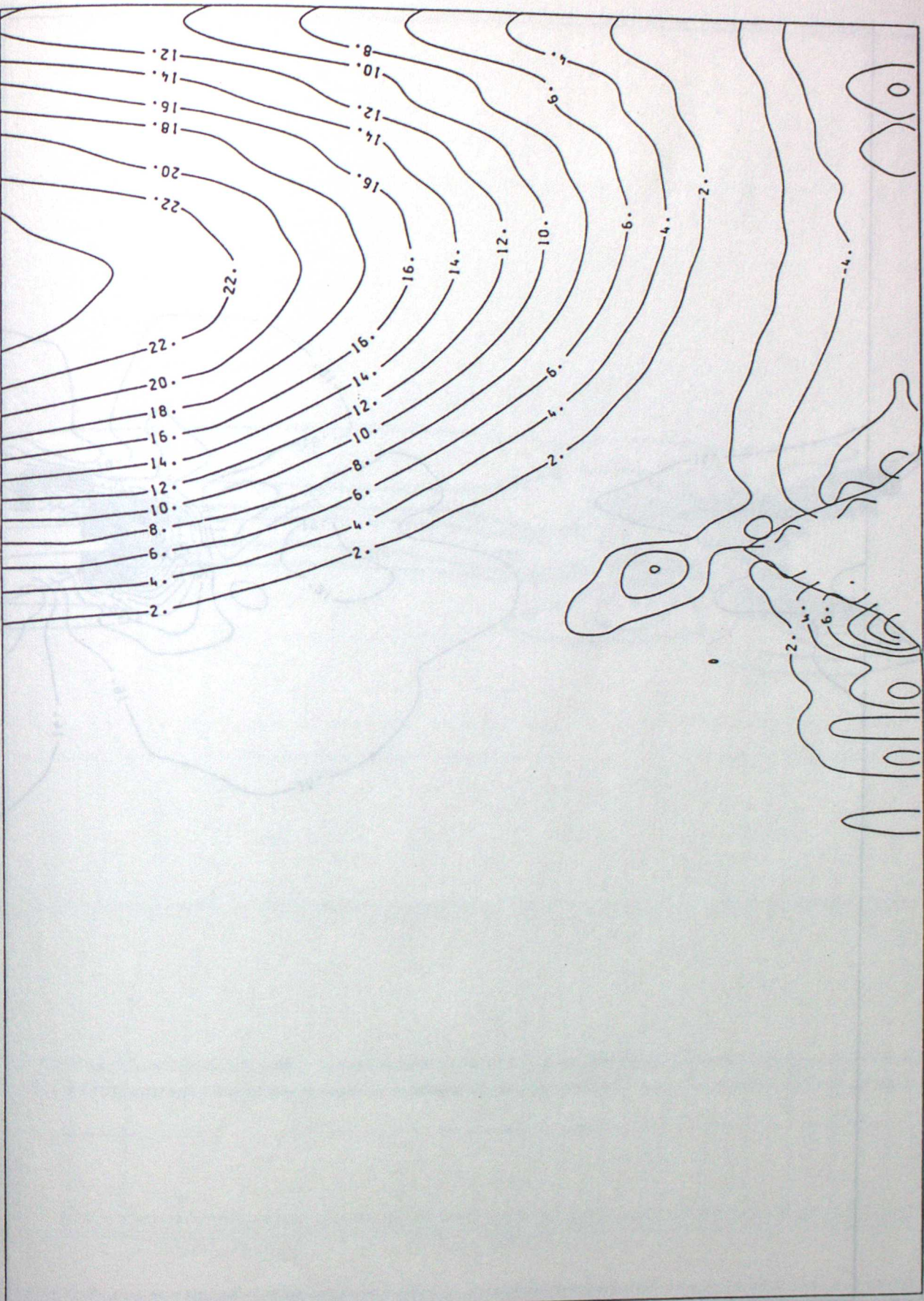


V AT T = 0.



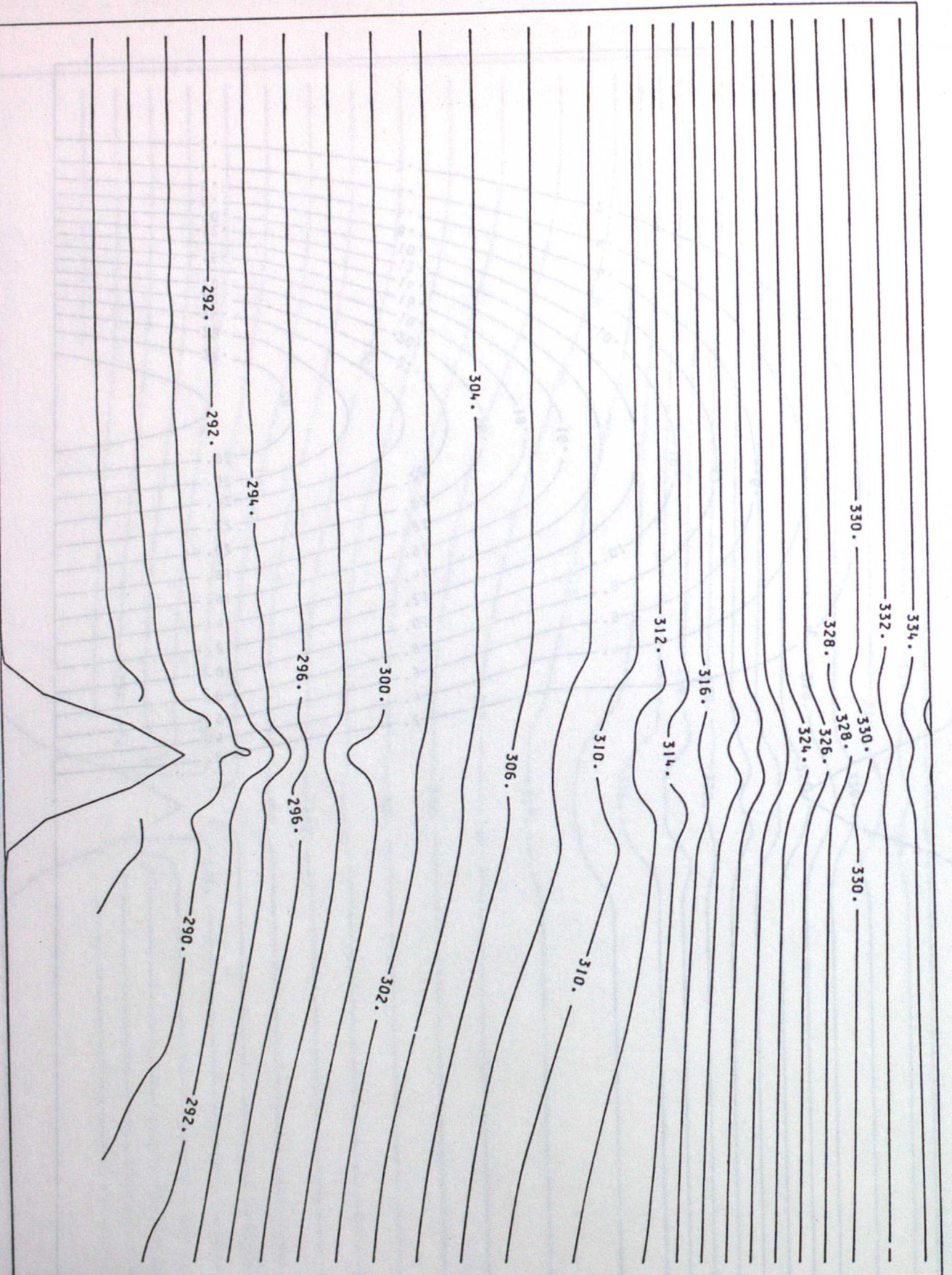
THETA AT T = 0.



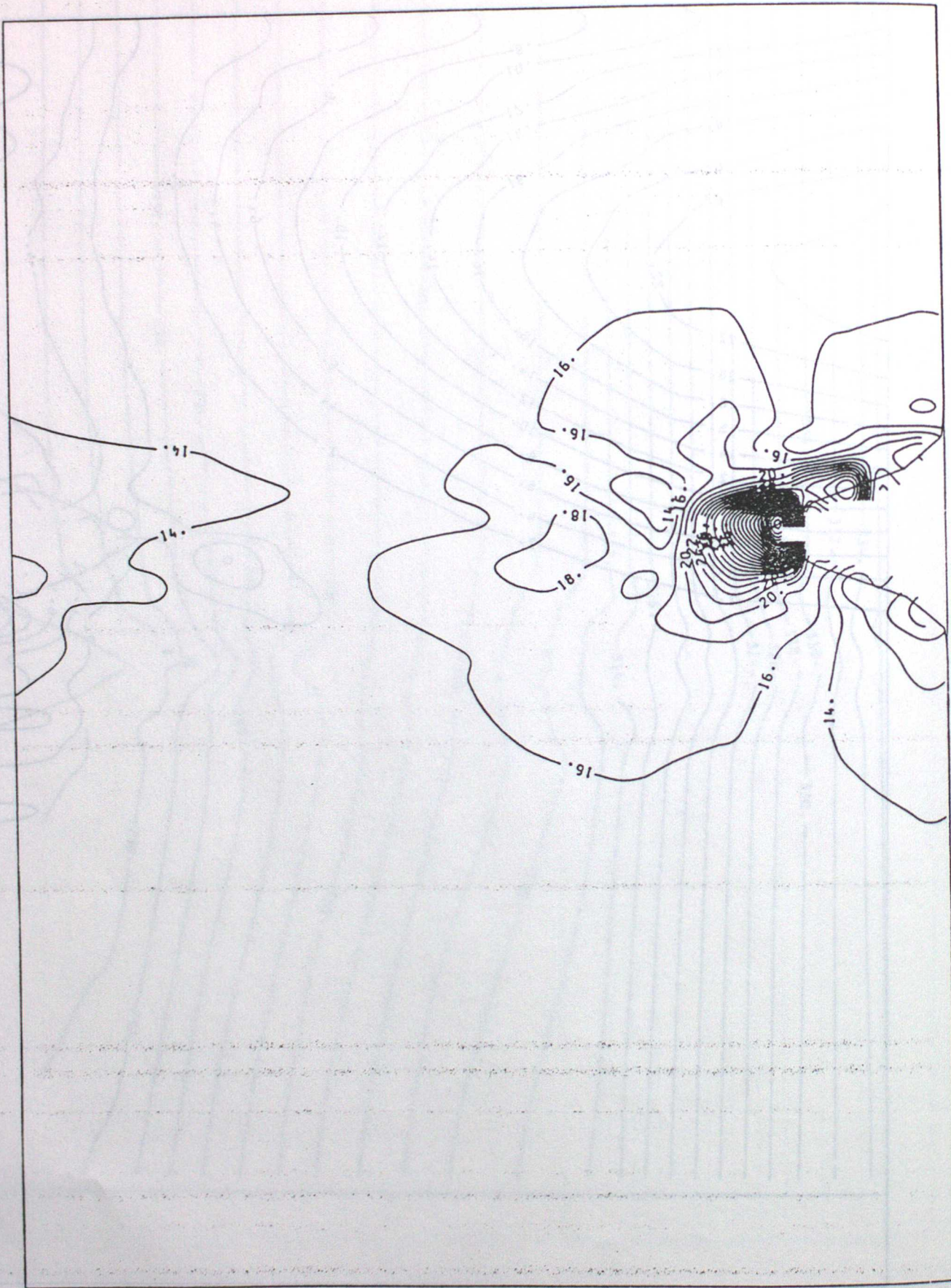


SMOOTH $\Delta t = 1$ HR Δ

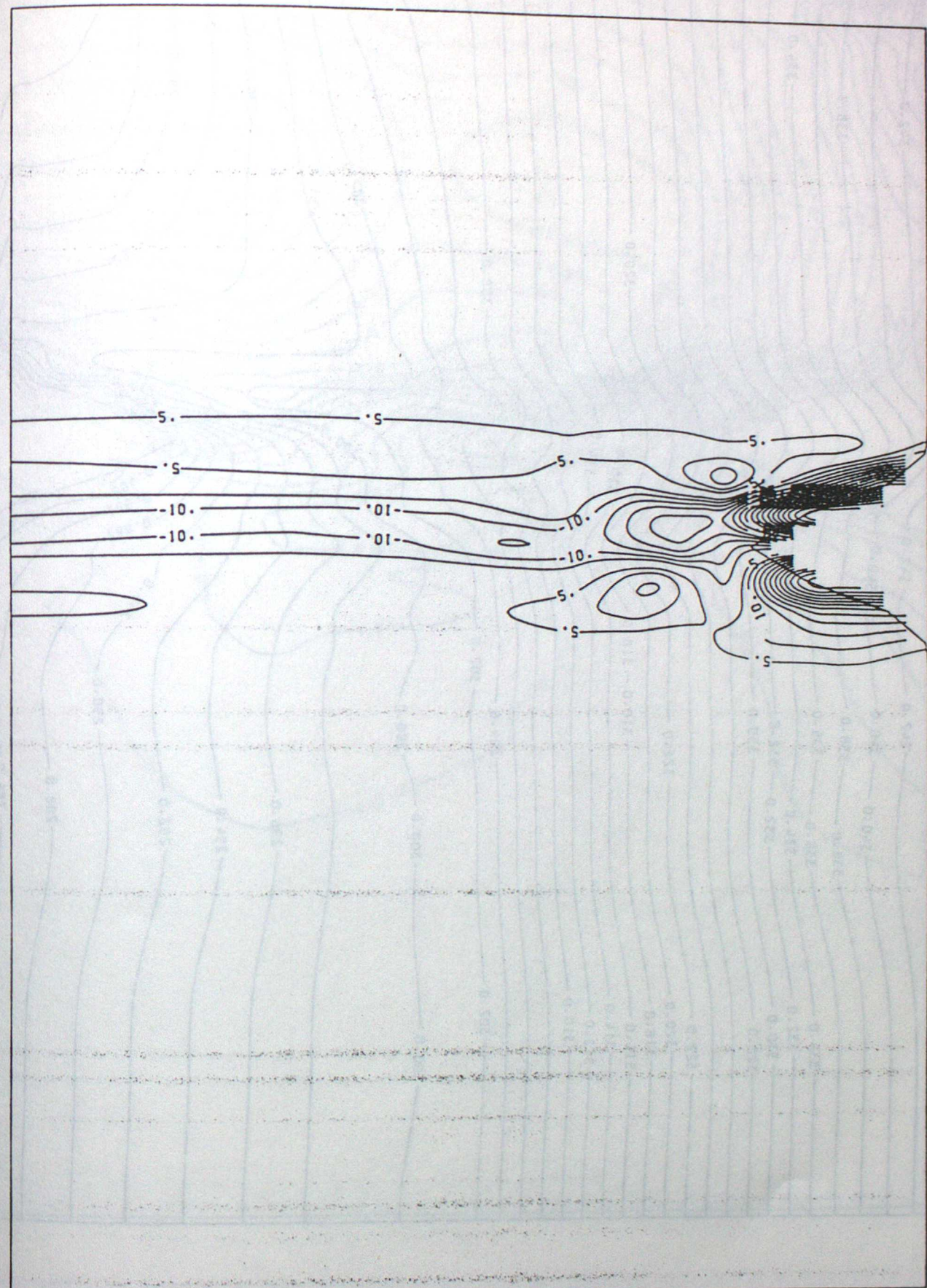
THEIR AT $t = 12$ hours



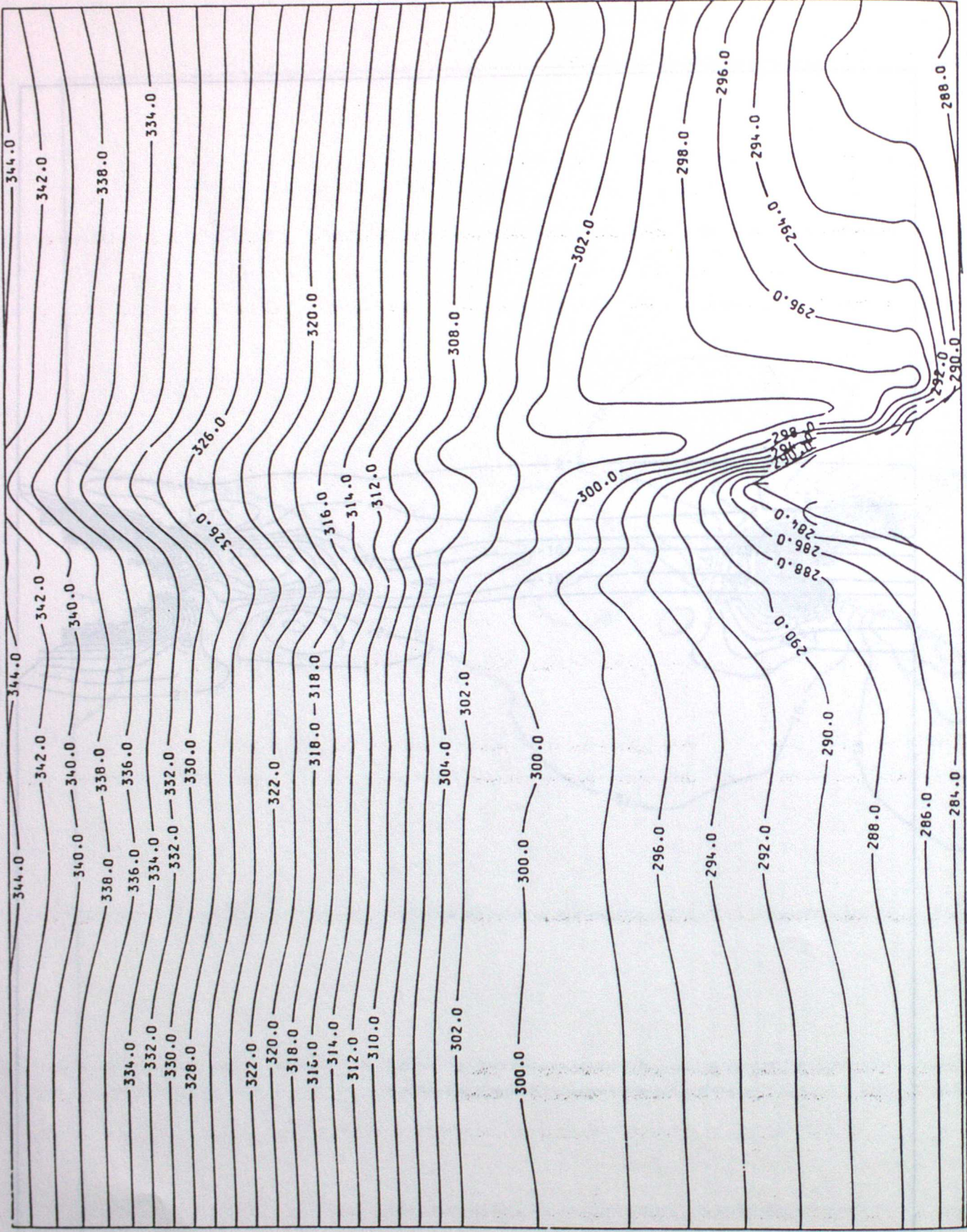
U AT T = 12 hours



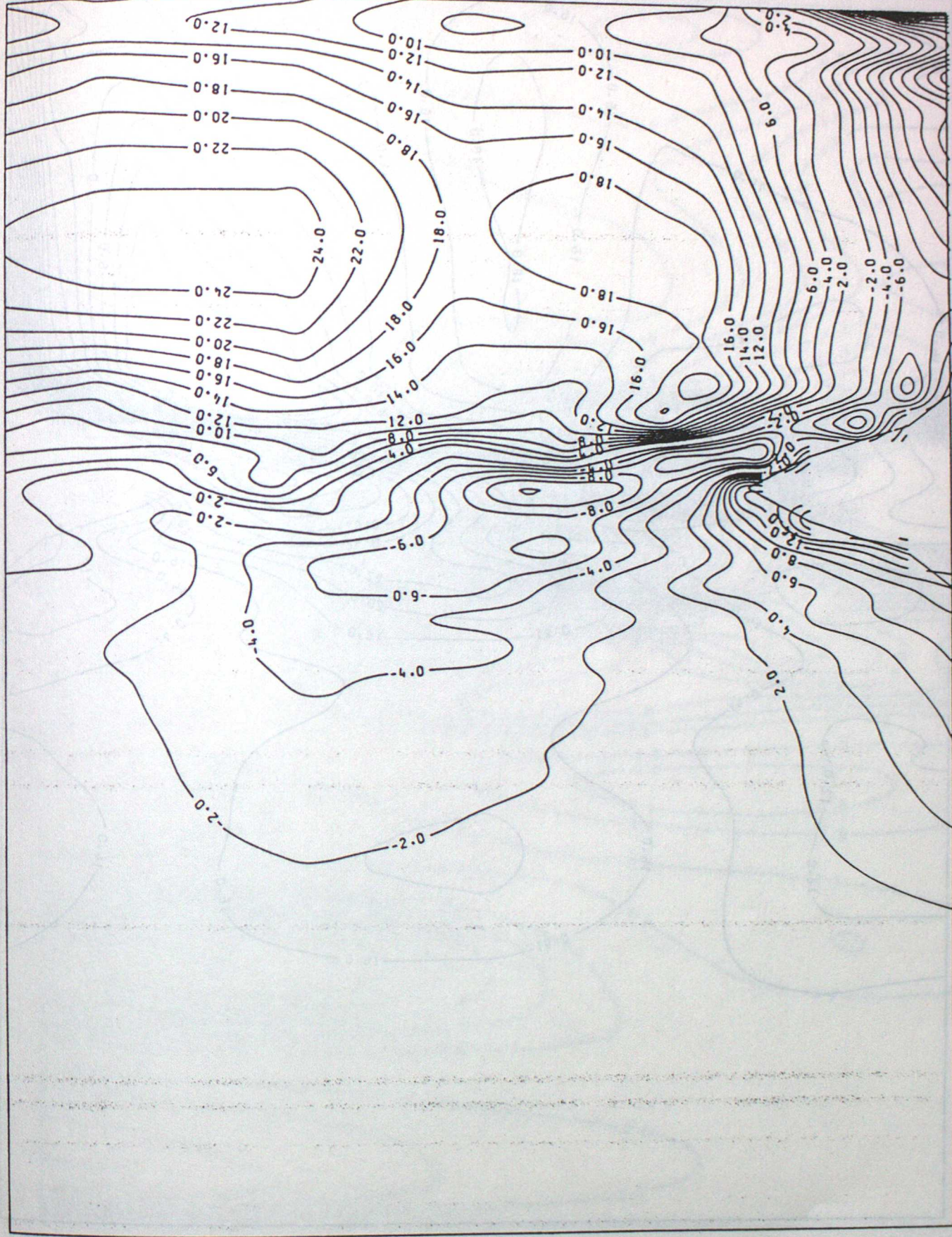
W (CH/S) AT T = 12 hours



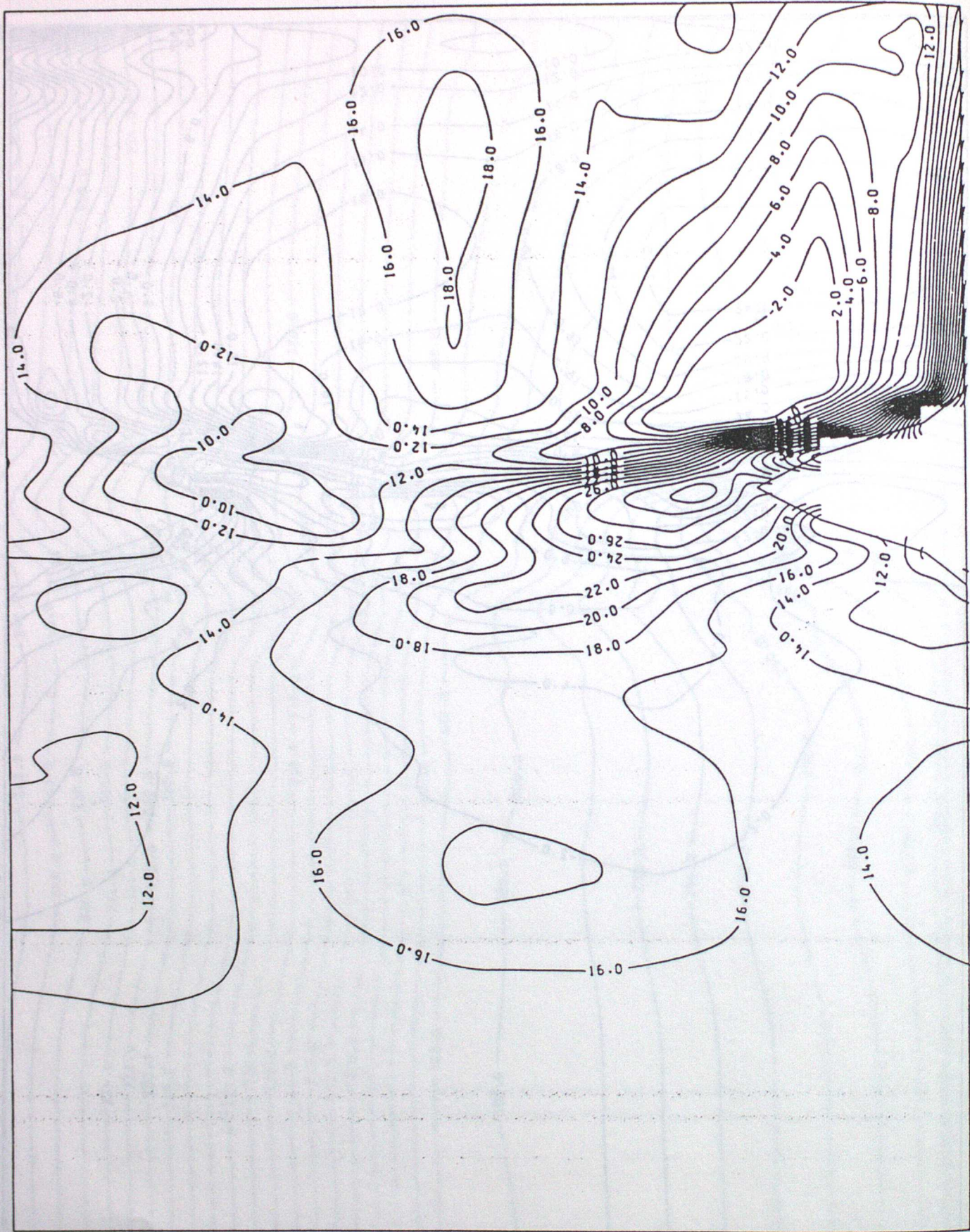
THETA AT T = 12 HOURS



V AT T = 12 HOURS



U AT T = 12 HOURS



W (CM/S) AT T = 12 HOURS

